

Optical spectroscopy of pure and doped CuGeO₃

A. Damascelli* and D. van der Marel

Solid State Physics Laboratory, University of Groningen, Nijenborgh 4, 9747 AG Groningen, The Netherlands

G. Dhahlenne and A. Revcolevschi

Laboratoire de Chimie des Solides, Université de Paris-sud, Bâtiment 414, F-91405 Orsay, France

(March 19, 1999)

We investigated in detail the optical properties of several Cu_{1- δ} Mg _{δ} GeO₃ (with $\delta=0, 0.01$), and CuGe_{1- x} B _{x} O₃ with B=Si ($x=0, 0.007, 0.05, 0.1$), and Al ($x=0, 0.01$) single crystals, in the frequency range 20-32 000 cm⁻¹. We report temperature dependent reflectivity and transmission measurements, performed with polarized light in order to probe the anisotropy of the crystals along the b and c axes, and optical conductivity spectra obtained by Kramers-Kronig transformation or direct inversion of the Fresnel formula. Special emphasis is given to the far-infrared phonon spectra. The temperature dependence of the phonon parameters is presented and discussed in relation to the soft mode issue in CuGeO₃. For $T < T_{\text{SP}}$ we could detect zone boundary folded modes activated by the spin-Peierls phase transition. Following the temperature dependence of these modes, which shows the second order character of the phase transition, we were able to study the effect of doping on T_{SP} . Moreover, in transmission experiments we detected a direct singlet-triplet excitation at 44 cm⁻¹, across the magnetic gap, which is not understandable on the basis of the magnetic excitation spectrum so far assumed for CuGeO₃. The optical activity of this excitation and its polarization dependence confirm the existence of a second (optical) magnetic branch, recently suggested on the basis of inelastic neutron scattering data. The anisotropy in the magnetic exchange constants along the b axis, necessary for the optical triplet mode to gain a finite intensity, and the strong effect of Si substitution on the phonon spectra are discussed in relation to the alternative space group $P2_12_12_1$, recently proposed for CuGeO₃ in the high temperature uniform phase.

I. INTRODUCTION

In 1993 Hase *et al.*¹ concluded, on the basis of magnetic susceptibility measurements, that CuGeO₃ is showing a spin-Peierls (SP) phase transition, i.e., a lattice distortion (due to the magneto-elastic coupling between the one-dimensional spin system and the three-dimensional phonon system) that occurs together with the formation of a spin-singlet ground state and the opening of a finite energy gap in the magnetic excitation spectrum. This magneto-elastic transition is driven by the magnetic energy gain due to dimerization of the antiferromagnetic (AF) exchange between the spin 1/2 moments of the Cu²⁺ ions [arranged in weakly coupled one-dimensional (1D) CuO₂ chains in this material²], which overcompensates the elastic energy loss resulting from the deformation of the lattice.^{3,4} In the SP ordered phase, the Cu²⁺ magnetic moments form singlet dimers along the chains and spin triplet excitations are gapped.¹

The SP nature of the phase transition in CuGeO₃ was inferred from the isotropic drop in the magnetic susceptibility at the transition temperature $T_{\text{SP}}=14$ K, and from the reduction of T_{SP} upon increasing the intensity of an applied magnetic field,¹ as theoretically expected for SP systems.³⁻⁶ This initial claim was later confirmed by an impressive variety of experimental results.⁷ The gap in the magnetic excitation spectrum was directly observed with inelastic neutron scattering,⁸ and the singlet-triplet nature of the gap was established with the same technique under application of a magnetic field: A splitting

of the single gap into three distinct excitation branches was clearly detected.⁹ The dimerization of the Cu²⁺ ions was observed and the lattice distortion very carefully investigated with both neutron and x-ray scattering.^{11,10,12} Finally, the phase transition from the dimerized to the incommensurate phase, expected in magnetic fields higher than a certain critical value,^{5,6} was found with field-dependent magnetization measurements at $H_c \approx 12$ T,¹³ and the H - T phase diagram was studied in great detail.¹⁴

The discovery of the SP phase transition in CuGeO₃ has renewed the interest in this phenomenon, observed previously in organic materials in the 1970's,¹⁵⁻¹⁷ because the availability of large high-quality single crystals of pure and doped CuGeO₃ made it possible to investigate this magneto-elastic transition by a very broad variety of experimental techniques. This way, the traditional SP theory based on 1D AF chains with only nearest-neighbor (nn) magnetic couplings and a mean-field treatment of the 3D phonon system,³⁻⁵ could be tested in all its expectations for a deeper understanding of the problem.

Also optical techniques, like Raman and infrared spectroscopy, are very useful in investigating magnetic and/or structural phase transitions. Information on the nature of the electronic (magnetic) ground state, lattice distortion and interplay of electronic (magnetic) and lattice degrees of freedom can be obtained studying in detail the electronic (magnetic) excitations and the phonon spectrum, as a function of temperature. The aim of our experimental investigation of CuGeO₃ with optical spec-

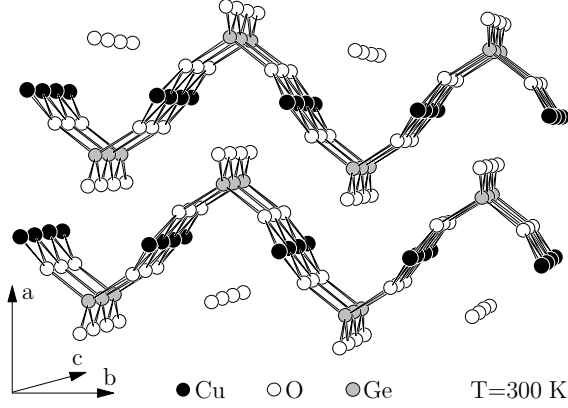


FIG. 1. Crystal structure of CuGeO_3 in the high temperature ($T=300$ K) undistorted phase.

troscopy was, of course, to detect all possible ‘infrared signatures’ of the SP phase transition in this material. However, we were in particular interested in a number of issues which could help us in understanding how far the classical SP picture^{3,4} is appropriate for the case of CuGeO_3 , namely:

(i) Analysis of the phonon spectra in order to study the lattice distortion and verify the proposed crystal structures for both the high and the low temperature phase.

(ii) Verify the presence of a soft mode in the phonon spectra, upon passing through the SP transition. In fact, a well-defined soft mode is expected in those theoretical models describing a SP system in terms of a linear coupling between lattice and magnetic degrees of freedom.^{5,4}

(iii) Detect possible magnetic bound states and/or a magnetic continuum in the excitation spectrum which could tell us about the symmetry and the order (nn versus nn) of the magnetic interactions.

(iv) Study the influence of doping on the vibrational and electronic properties.

Before proceeding to the experimental results, we will present in the next section the outcome of a group theoretical analysis, which will be useful in the discussion of the phonon spectra. In fact, the number and the symmetry of the infrared and Raman active phonons expected for the proposed high-temperature undistorted phase² and the low-temperature SP phase^{11,12} of CuGeO_3 can be obtained from a group theoretical analysis of the lattice vibrational modes.¹⁸ The results of this calculation will later be compared to the experimental data.

II. GROUP THEORETICAL ANALYSIS

At room temperature the orthorhombic crystal structure with lattice parameters $a=4.81$ Å, $b=8.47$ Å, and $c=2.941$ Å and space group $Pbmm$ ($x||a, y||b, z||c$) or, equivalently, $Pmma$ ($x||b, y||c, z||a$) in standard setting, was proposed for CuGeO_3 .² The building blocks of the structure are edge-sharing CuO_6 octahedra and corner-

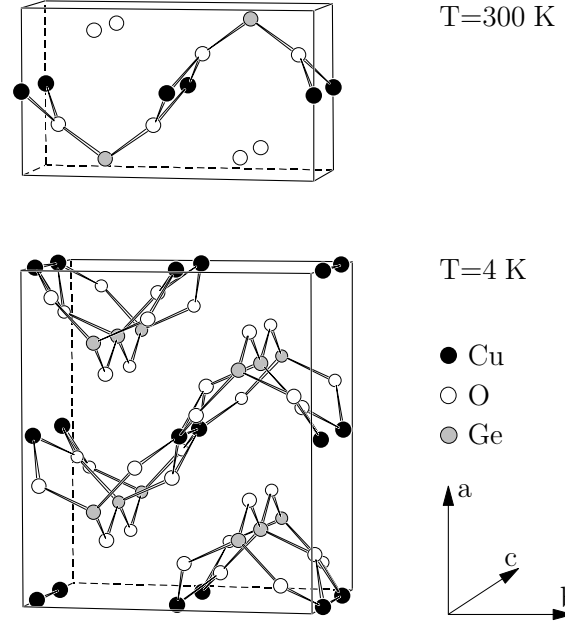


FIG. 2. Conventional unit cell of CuGeO_3 in the undistorted (top) and SP phase (bottom). For clarity purpose, the ion displacements due to the SP transition have been enlarged by a factor of 30.

sharing GeO_4 tetrahedra stacked along the c axis of the crystal and resulting in Cu^{2+} and Ge^{4+} chains parallel to the c axis. These chains are linked together via the O atoms, and form layers parallel to the b - c plane weakly coupled along the a axis (Fig. 1). The unit cell contains 2 formula units of CuGeO_3 (Fig. 2), with site group C_{2h}^y for the 2 Cu atoms, C_{2v}^z for the 2 Ge and the 2 O(1) atoms, and C_s^{xz} for the 4 O(2) atoms [where O(2) denotes the O atoms linking the chains together].^{11,12} A group theoretical analysis can be performed, working in standard orientation, to obtain the number and the symmetry of the lattice vibrational modes. Following the nuclear site group analysis method extended to crystals,¹⁹ the contribution of each occupied site to the total irreducible representation of the crystal is:

$$\Gamma_{\text{Cu}} = A_u + 2B_{1u} + B_{2u} + 2B_{3u},$$

$$\Gamma_{\text{Ge+O(1)}} = 2[A_g + B_{1u} + B_{2g} + B_{2u} + B_{3g} + B_{3u}],$$

$$\Gamma_{\text{O(2)}} = 2A_g + A_u + B_{1g} + 2B_{1u} + 2B_{2g} + B_{2u} + B_{3g} + 2B_{3u}.$$

Subtracting the silent modes ($2A_u$) and the acoustic modes ($B_{1u} + B_{2u} + B_{3u}$), the irreducible representation of the optical vibrations in standard setting ($Pmma$), is:

$$\Gamma = 4A_g(aa, bb, cc) + B_{1g}(bc) + 4B_{2g}(ab) + 3B_{3g}(ac) + 5B_{1u}(E||a) + 3B_{2u}(E||c) + 5B_{3u}(E||b). \quad (1)$$

This corresponds to an expectation of 12 Raman active modes ($4A_g + B_{1g} + 4B_{2g} + 3B_{3g}$) and 13 infrared active modes ($5B_{1u} + 3B_{2u} + 5B_{3u}$) for CuGeO_3 , in agreement with the calculation done by Popović *et al.*²⁰

At temperatures lower than T_{SP} the proposed crystal structure is still orthorhombic, but with lattice parameters $a' = 2 \times a$, $b' = b$ and $c' = 2 \times c$ and space group $Bbcm$ ($x||a$, $y||b$, $z||c$) or, equivalently, $Cmca$ ($x||c$, $y||a$, $z||b$) in standard setting.^{11,12} The distortion of the lattice taking place at the phase transition (Fig. 2) is characterized by the dimerization of Cu-Cu pairs along the c axis (dimerization out of phase in neighboring chains), together with a rotation of the GeO_4 tetrahedra around the axis defined by the O(1) sites (rotation opposite in sense for neighboring tetrahedra). Moreover, the O(2) sites of the undistorted structure split in an equal number of O(2a) and O(2b) sites, distinguished by the distances O(2a)-O(2a) and O(2b)-O(2b) shorter and larger than O(2)-O(2),¹² respectively. The SP transition is also characterized (Fig. 2) by a doubling of the unit cell (corresponding to a doubling of the degrees of freedom from 30 to 60). The site groups in the new unit cell are: C_2^x for Cu, C_2^y for O(1), and C_s^{yz} for Ge, O(2a) and O(2b).¹² Repeating the group theoretical analysis, we obtain for the contributions to the total irreducible representation:

$$\begin{aligned}\Gamma_{\text{Cu}} &= A_g + A_u + 2B_{1g} + 2B_{1u} + 2B_{2g} + 2B_{2u} + B_{3g} + B_{3u}, \\ \Gamma_{\text{O(1)}} &= A_g + A_u + 2B_{1g} + 2B_{1u} + B_{2g} + B_{2u} + 2B_{3g} + 2B_{3u}, \\ \Gamma_{\text{Ge+O(2a)+O(2b)}} &= 3[2A_g + A_u + B_{1g} + 2B_{1u} + B_{2g} \\ &\quad + 2B_{2u} + 2B_{3g} + B_{3u}].\end{aligned}$$

The irreducible representation of the optical vibrations of CuGeO_3 in the SP phase in standard setting ($Cmca$), is:

$$\begin{aligned}\Gamma_{\text{SP}} &= 8A_g(aa, bb, cc) + 7B_{1g}(ac) + 6B_{2g}(bc) + 9B_{3g}(ab) \\ &\quad + 9B_{1u}(E||b) + 8B_{2u}(E||a) + 5B_{3u}(E||c).\end{aligned}\quad (2)$$

Therefore 30 Raman active modes ($8A_g + 7B_{1g} + 6B_{2g} + 9B_{3g}$) and 22 infrared active modes ($9B_{1u} + 8B_{2u} + 5B_{3u}$) are expected for CuGeO_3 in the SP phase, all the additional vibrations being zone boundary modes activated by the folding of the Brillouin zone.

In order to compare the results obtained for the undistorted and the SP phase of CuGeO_3 , it is better to rewrite the irreducible representations Γ and Γ_{SP} into $Pbmm$ and $Bbcm$ settings, respectively, because both groups are characterized by: $x||a$, $y||b$ and $z||c$. This can be done by permuting the $(1g, 2g, 3g)$ and $(1u, 2u, 3u)$ indices in such a way that it corresponds to the permutations of the axis relating $Pmma$ to $Pbmm$, and $Cmca$ to $Bbcm$. Therefore, the irreducible representations of the optical vibrations of CuGeO_3 , for $T > T_{\text{SP}}$ ($Pbmm$) and $T < T_{\text{SP}}$ ($Bbcm$), respectively, are:

$$\begin{aligned}\Gamma' &= 4A_g(aa, bb, cc) + 4B_{1g}(ab) + 3B_{2g}(ac) + B_{3g}(bc) \\ &\quad + 3B_{1u}(E||c) + 5B_{2u}(E||b) + 5B_{3u}(E||a),\end{aligned}\quad (3)$$

$$\begin{aligned}\Gamma'_{\text{SP}} &= 8A_g(aa, bb, cc) + 9B_{1g}(ab) + 7B_{2g}(ac) + 6B_{3g}(bc) \\ &\quad + 5B_{1u}(E||c) + 9B_{2u}(E||b) + 8B_{3u}(E||a).\end{aligned}\quad (4)$$

It is now evident that the number of infrared active phonons is expected to increase from 5 to 8, 5 to 9 and 3 to 5 for light polarized along the a , b and c axes, respectively.

III. EXPERIMENTAL

We investigated the optical properties of several $\text{Cu}_{1-\delta}\text{Mg}_\delta\text{GeO}_3$ (with $\delta = 0, 0.01$), and $\text{CuGe}_{1-x}\text{B}_x\text{O}_3$ [with $B=\text{Si}$ ($x = 0, 0.007, 0.05, 0.1$), and Al ($x = 0, 0.01$)] single crystals, in the frequency range 20-32000 cm^{-1} . These high-quality single crystals, several centimeters long in the a direction, were grown from the melt by a floating zone technique.²¹ Plate-like samples were easily cleaved perpendicularly to the a axis. Typical dimensions were about 2 and 6 mm parallel to the b and c axis, respectively. The thickness was chosen in dependence of the experiment to be performed. In reflectivity measurements, when enough material was available, several millimeters thick samples were used in order to avoid interference fringes in the spectra, due to Fabry-Perot resonances.²² Particular attention had to be paid when measuring reflectivity in frequency regions characterized by weak excitations (i.e., from 1000 to 25000 cm^{-1}): Because of the multiple reflections within the sample these excitations, which would not be directly detectable in reflectivity, would be observable as an absorption with respect to the background dominated by the interference fringes. If a Kramers-Kronig transformation is performed on such a pathological data in order to obtain the optical conductivity, unphysical results would be produced. As a matter of fact, it is precisely for this reason that a charge-transfer excitation at 1.25 eV (10000 cm^{-1}) was erroneously reported in one of the early optical papers on CuGeO_3 .²³ On the other hand, in transmission measurements, where interference fringes cannot be avoided, the thickness of the sample was adjusted to the strength of the particular excitation under investigation.

The samples were aligned by conventional Laue diffraction and mounted in a liquid He flow cryostat to study the temperature dependence of the optical properties between 4 and 300 K. Reflectivity and transmission measurements in the frequency range going from 20-7000 cm^{-1} were performed with a Fourier transform spectrometer (Bruker IFS 113v), with polarized light, in order to probe the optical response of the crystals along the b and the c axes. In reflectivity a near normal incidence configuration ($\theta = 11^\circ$) was used. The absolute reflectivity and transmission values were obtained by calibrating the data acquired on the samples against a gold mirror and an empty sample holder, respectively. For frequencies higher than 6000 cm^{-1} a Woollam (VASE) ellipsometer was used in both transmission and reflection operational modes. Unfortunately, on this last system it was not possible to perform temperature dependent measurements. The optical conductivity spectra were obtained

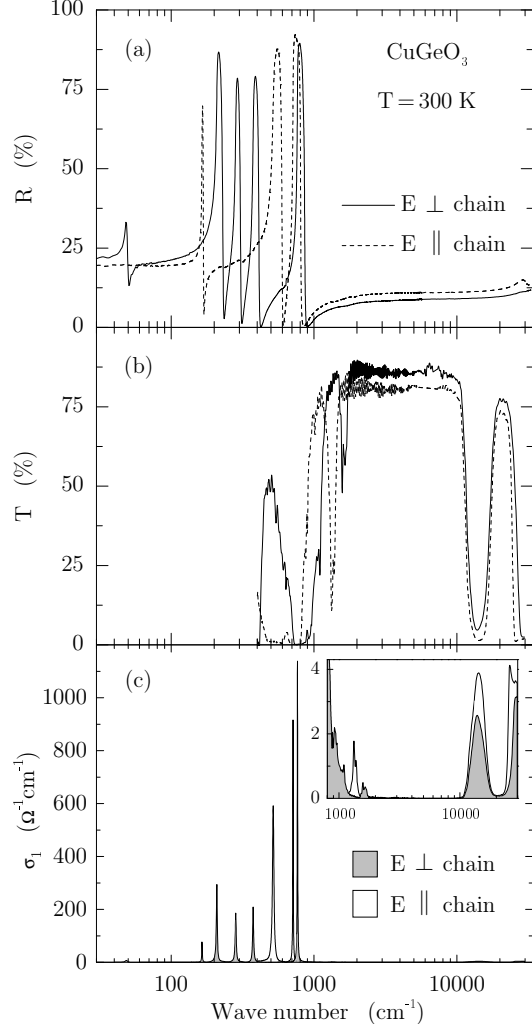


FIG. 3. Optical spectra of CuGeO_3 at 300 K for $E \parallel b$ (i.e., \perp to the chain direction) and $E \parallel c$ (i.e., \parallel to the chain direction), in the frequency range going from 30 to 34000 cm^{-1} . Panel (a), (b), and (c) show the results for reflectivity, transmission, and optical conductivity, respectively. In the inset of panel (c) an enlarged view of $\sigma_1(\omega)$ from 800 to 30000 cm^{-1} is presented (note the very low absolute value of conductivity).

by Kramers-Kronig transformations in the regions where only reflectivity spectra were measurable, and by direct inversion of the Fresnel equations wherever both reflection and transmission data were available.²²

IV. PURE CuGeO_3

Let us now, as an introduction to what we will discuss in detail in the following sections, describe briefly the main features of the optical spectra of pure CuGeO_3 over the entire frequency range we covered with our experimental systems. In Fig. 3 we present reflectivity, transmission, and conductivity spectra of CuGeO_3 at 300 K, for $E \parallel b$ (i.e., \perp to the chain direction), and $E \parallel c$ (i.e., \parallel

to the chain direction), in the frequency range going from 30 to 34000 cm^{-1} . The results are typical of an ionic insulator. The far-infrared region ($\omega < 1000 \text{ cm}^{-1}$) is characterized by strong optical phonon modes showing the expected anisotropy for the b and c axes, as one can see from reflectivity and conductivity (the detail discussion of the phonon spectra will be subject of the next section). Besides the phonon lines, no background conductivity is observable (Fig. 3c). Transmission spectra for $\omega < 400 \text{ cm}^{-1}$ are not shown. However, infrared transmission measurements carried out at low temperature, in order to investigate very weak magnetic and lattice excitations, will be discussed later in the course of the paper. At frequencies larger than 1000 cm^{-1} , reflectivity is low and almost completely featureless. More information can be gained from transmission in this case. In Fig. 3b we can see (in addition to the strong phonons for $\omega < 1000 \text{ cm}^{-1}$) absorption processes at 1330 and 1580 cm^{-1} along the c and b axes, respectively, and at ~ 14000 and $\sim 27000 \text{ cm}^{-1}$, with approximately the same frequency for the two different axes. Having both reflectivity and transmission data in this region, we could calculate the dynamical conductivity by direct inversion of the Fresnel formula.²² As shown by Fig. 3c and, in particular, by the enlarged view given in the inset (note the very low absolute value of conductivity), extremely weak excitations are present, in the region going from 1000 to 30000 cm^{-1} , on top of a zero background. Let us now briefly discuss the nature of these excitations. At 1000 cm^{-1} we can see the vanishing tail of the highest b -axis phonon (inset of Fig. 3c). Above that, we find the two peaks at 1330 and 1580 cm^{-1} along the c and b axes, respectively. On the basis of the energy position and of the temperature dependence, these features can be ascribed to multiphonon processes. At $\sim 14000 \text{ cm}^{-1}$ ($\sim 1.8 \text{ eV}$), for both orientations of the electric field, a very weak peak is present which has been shown to be due to phonon-assisted Cu d - d transitions.²⁴ Finally, the onset of the Cu-O charge-transfer excitations is observable at $\sim 27000 \text{ cm}^{-1}$. Superimposed to it are some sharper features of probable excitonic nature.

A. Phonon Spectrum and Lattice Distortion

In this section we will discuss in detail the phonon spectrum of pure CuGeO_3 , for both the high temperature undistorted phase and the low temperature dimerized SP phase. In particular, we will analyze the optical data in order to find possible zone-boundary folded modes activated by the lattice distortion involved in the SP phase transition. The c and b -axis (i.e., $E \parallel \text{chain}$ and $E \perp \text{chain}$, respectively) reflectivity spectra of CuGeO_3 in the undistorted phase are presented in Fig. 4, for two different temperatures higher than $T_{\text{SP}} = 14 \text{ K}$. The data are shown up to 1000 cm^{-1} which covers the full phonon spectrum. Three phonons are detected along the c axis ($\omega_{\text{TO}} \approx 167, 528$ and 715 cm^{-1} , for $T = 15 \text{ K}$), and five

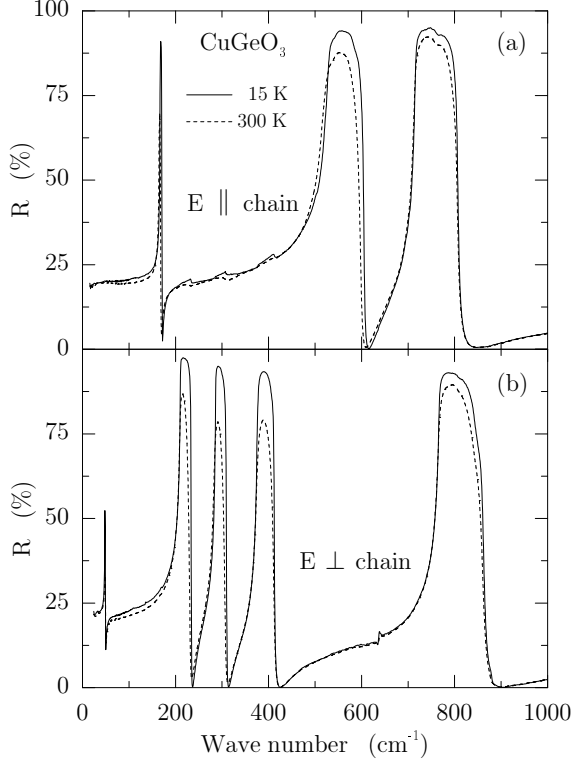


FIG. 4. Reflectivity of a single crystal of pure CuGeO_3 , as a function of frequency, at two different temperatures (300 K and 15 K) in the undistorted phase. The spectra are shown for E parallel and perpendicular to the chain direction in panel (a) and (b), respectively.

along the b axis ($\omega_{\text{TO}} \approx 48, 210, 286, 376$ and 766 cm^{-1} , for $T = 15 \text{ K}$). This is in agreement with what is expected on the basis of the group-theoretical analysis presented in section II, (see Eq. 3) for the space group $Pbmm$ proposed for CuGeO_3 in the uniform phase.² The structure in Fig. 4a between 200 and 400 cm^{-1} is due to a leakage of the polarizer and corresponds to the three modes detected along the b axis in the same frequency range. Similarly, the feature at approximately 630 cm^{-1} in Fig. 4b is a leakage of a mode polarized along the a axis.²⁰ However, the reason why this phonon has been detected in the b -axis reflectivity is not simply, as in the previous case, a leakage of the polarizer. It has to do with the finite angle of incidence $\theta = 11^\circ$ of the radiation on the sample, and with the fact that p -polarized light was used to probe the optical response along the b axis. In fact, whereas for s -polarized light the electric field was parallel to the b - c plane, in p polarization there was a small but finite component of the electric vector perpendicular to the plane of the sample, which could then couple to the a -axis excitations (at least to those particularly intense). As a last remark, we would like to stress that the temperature dependence observable in the reflectivity spectra of Fig. 4 mainly corresponds to the hardening and sharpening of the phonon lines, usually observable

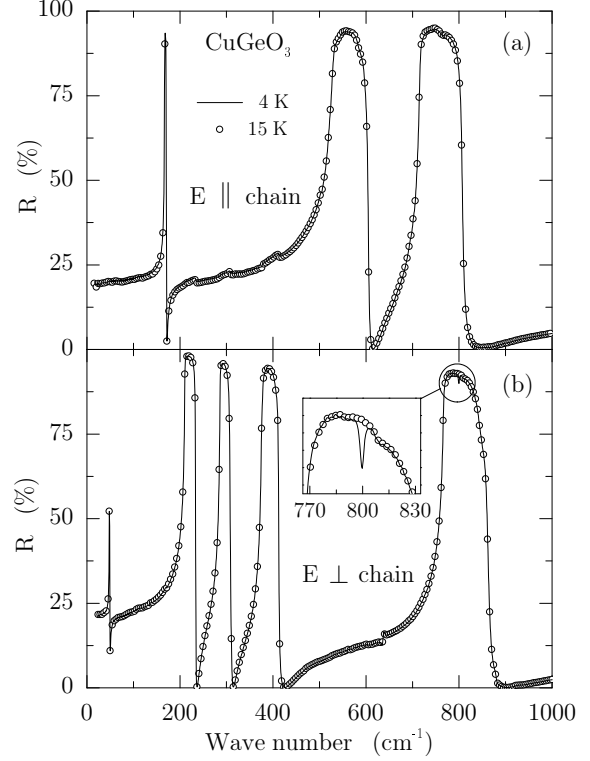


FIG. 5. Comparison between reflectivity spectra measured in the SP phase at 4 K (solid line) and just before the SP transition at 15 K (circles) on a pure single-crystal of CuGeO_3 . For $E \parallel \text{chain}$ (a) no difference is found across the phase transition whereas for $E \perp \text{chain}$ (b) a new feature appears at 800 cm^{-1} (as clearly shown in the inset).

in a crystalline material upon reducing the temperature. However, a more extensive discussion of the temperature dependence of the phonon parameters over a broad temperature range will be presented in section IV B, in relation to the soft-mode issue.

Cooling down the sample below the phase transition temperature $T_{\text{SP}} = 14 \text{ K}$, we can seek for changes in the phonon spectrum with respect to the result obtained at temperature just above T_{SP} . The c and b -axis reflectivity spectra measured at $T = 15 \text{ K}$ (circles) and $T = 4 \text{ K}$ (solid line) are compared in Fig. 5. The 15 K curves have been plotted with lower resolution, for the sake of clarity. The solid line is the 4 K experimental result. Whereas for $E \parallel c$ the spectra are exactly identical, a new feature, though very weak, is detected in the SP phase at 800 cm^{-1} for $E \parallel b$, as shown in the inset of Fig. 5b. A careful investigation of temperatures ranging from 4 to 15 K (see Fig. 6) clearly shows that this feature, that falls in the frequency region of high reflectivity for the B_{2u} -symmetry mode at 766 cm^{-1} and therefore shows up mainly for its absorption, is activated by the SP transition.²⁵ It corresponds to a new peak in conductivity, superimposed on the background due to the lorentzian tail of the close B_{2u} phonon (see inset of Fig. 6).

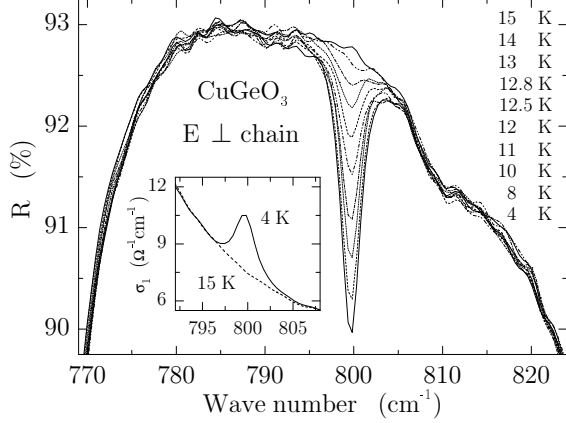


FIG. 6. Detailed temperature dependence of the 800 cm^{-1} line observed with $E \perp \text{chain}$ in the reflectivity spectra for $T < T_{\text{SP}}$. In the inset, where the dynamical conductivity calculated via Kramers-Kronig analysis is plotted, a new peak is clearly visible for $T = 4 \text{ K}$.

By fitting the reflectivity spectra with Lorentz oscillators for all the optical phonons, it is possible to obtain the temperature dependence of the oscillator strength for the 800 cm^{-1} feature. The results are plotted in Fig. 7, together with the peak intensity of a superlattice reflection measured by Harris *et al.*²⁶ in an x-ray scattering experiment on a pure CuGeO_3 single crystal characterized, as our sample, by $T_{\text{SP}} \approx 13.2 \text{ K}$. The data clearly show the second-order character of the phase transition. From the perfect agreement of the infrared and x-ray scattering results, and from the observation that the resonant frequency is not shifting at all with temperature, we can conclude that the peak at 800 cm^{-1} corresponds to a pure lattice excitation. It has to be a folded zone-boundary mode most probably related to the B_{2u} phonon observed at 766 cm^{-1} , which is mainly an oxygen vibration.²⁰ We can then estimate for the B_{2u} mode an energy dispersion, over the full Brillouin zone, of the order of $34 \text{ cm}^{-1} = 4.22 \text{ meV}$, at $T = 15 \text{ K}$. If magnetic degrees of freedom were involved (e.g., if this excitation were a magnon-plus-phonon process²⁷), not only a decrease in intensity would be observable, but also a frequency shift to lower values, reflecting the closing of the magnetic gap for $T \rightarrow T_{\text{SP}}$ from below. In fact, on the basis of Cross and Fisher theory,⁴ the magnetic gap would scale as $\delta^{2/3}$ [where $\delta \sim (1 - T/T_{\text{SP}})^\beta$, close to T_{SP} , denotes the generalize symmetry-breaking lattice distortion]. Its gradual closing has been directly observed in neutron and inelastic light scattering experiments.^{28,29}

Because both the intensity of the superlattice reflections measured with x-ray or neutron scattering, and the intensity of the zone-boundary folded modes in an optical experiment are proportional to δ^2 (see Ref. 30), we can try to fit the temperature dependence of the oscillator strength for the 800 cm^{-1} SP-activated mode to the equation $\sim (1 - T/T_{\text{SP}})^{2\beta}$. As a result of the fit per-

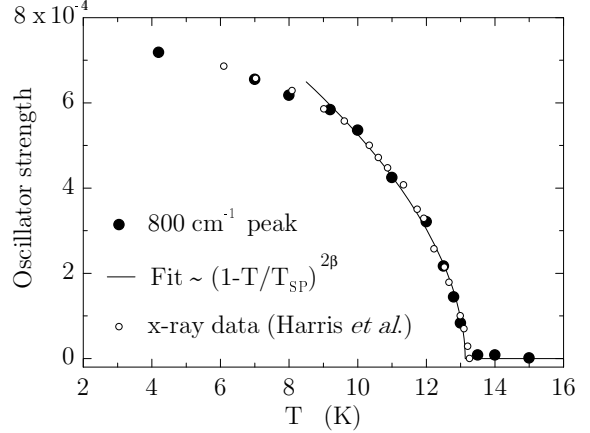


FIG. 7. Oscillator strength of the 800 cm^{-1} folded mode, observed for $E \perp \text{chain}$ on a pure CuGeO_3 single crystal, plotted versus temperature. The x-ray scattering data of Harris *et al.*²⁶ and the fit to a power law in the reduced temperature are also shown.

formed over a broad temperature range (see Fig. 7), we obtained $\beta = 0.26 \pm 0.02$, in agreement with Ref. 28. However, the best fit value of β is strongly dependent on the temperature range chosen to fit the data.³¹ If only points very close (within 1 K) to T_{SP} are considered, the value $\beta = 0.36 \pm 0.03$ is obtained, as reported in Ref. 32. At this point, in relation to the soft-mode issue in CuGeO_3 treated in section IV B, it is worth mentioning that for the organic SP system $\text{TTF-CuS}_4\text{C}_4(\text{CF}_3)_4$, which shows a precursive 3D soft-phonon at the superlattice position, the value $\beta = 0.5$ was obtained.³³ It was argued by Cross and Fisher,⁴ that this soft-mode is responsible for the mean-field behavior, i.e. $\beta = 1/2$, in the TTF salt.

As we saw in Fig. 5, only one phonon activated by the SP phase transition, of the many we actually expected, is directly observable in reflectivity spectra. However, more lines can be found by means of a deeper analysis, in agreement with the results reported in Ref. 34. In fact, by checking the optical conductivity at 4 and 15 K, a second folded mode is found along the b axis at 310 cm^{-1} (see Fig. 8). This line was not distinguishable in reflectivity because it coincides with ω_{LO} of the B_{2u} -symmetry phonon at 286 cm^{-1} . The reasons for not detecting all the phonons predicted from the group theoretical analysis (Eq. 4) in reflectivity measurements, at $T < T_{\text{SP}}$, are probably the small values of the atomic displacements involved in the SP transition (with a correspondingly small oscillator strength of zone-boundary modes), and/or possibly the small dispersion of the optical branches of some of the lattice vibrations. However, it is not surprising that the only activated modes have been detected along the b axis of the crystal: for this particular direction, below the phase transition, a strong spontaneous thermal contraction has been observed,²⁸ which can be responsible for a relative increase of the oscillator strength of the phonons polarized along the b axis, with respect to those

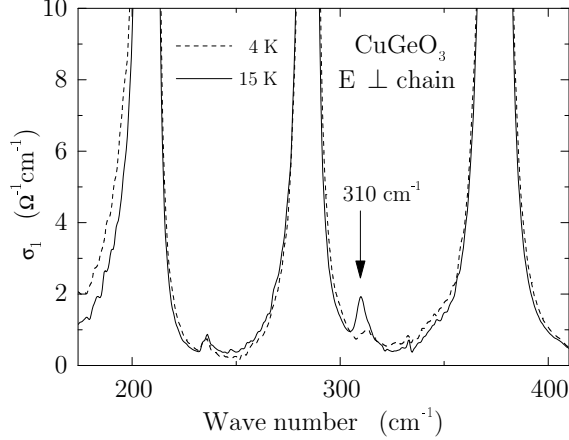


FIG. 8. Comparison between conductivity spectra measured in the SP phase at 4 K and just before the SP transition at 15 K, for $E \perp$ chain, on a pure single-crystal of CuGeO_3 : A zone boundary folded mode appears, across the phase transition, at 310 cm^{-1} .

polarized along the c axis.

In order to probe the phonon spectrum of the dimerized phase with a more sensitive tool, we performed transmission measurements on a $350 \mu\text{m}$ thick sample, in the far-infrared region. One more line was then detected at 284 cm^{-1} along the c axis, as shown in Fig. 9. In the top panel a transmission spectrum acquired at 4 K is plotted in the frequency range $100\text{-}300 \text{ cm}^{-1}$. Fabry-Perot interference fringes are clearly visible, interrupted at $\sim 167 \text{ cm}^{-1}$ by the strong absorption of the lowest energy B_{1u} -symmetry phonon. Moreover, at 284 cm^{-1} one can observe a slightly more pronounced minimum in the interference pattern. However, because of the weakness of this line, a real peak can be observed only in the absorbance difference spectrum (bottom panel of Fig. 9). The spikes present at $\sim 167 \text{ cm}^{-1}$ in the absorbance difference spectrum are due to the complete absorption of the light in that frequency range (top panel). As a last remark, we want to stress that the final assignment of the 310 and 284 cm^{-1} peaks to optical phonons activated by the SP transition is based, as for the line at 800 cm^{-1} , on their detailed temperature dependence (not shown).

B. Phonon Parameters and Soft-Mode Issue

As far as the dynamical interplay between spins and phonons in CuGeO_3 is concerned, it is clear from the reflectivity spectra plotted in Fig. 4 and 5 that a well-defined soft mode, driving the structural deformation in CuGeO_3 , has not been detected in our measurements. However, as any dimerization must be related to normal modes away from the zone center, the softening of one or more modes, across the SP phase transition, should be expected at $k = (\pi/a, 0, \pi/c)$, the actual propagation vector in CuGeO_3 . As optical techniques can probe the phonon

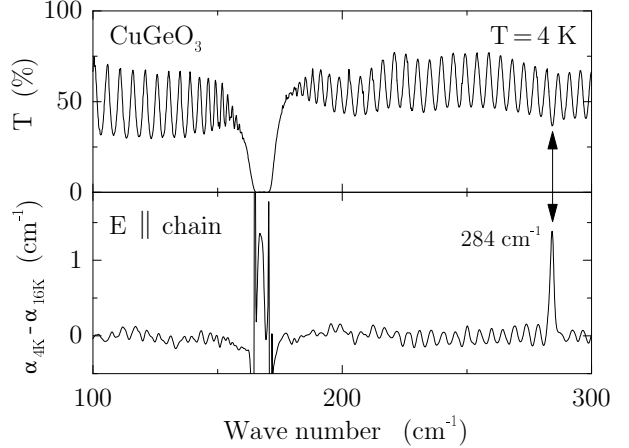


FIG. 9. Top panel: Transmission spectrum of a pure single-crystal of CuGeO_3 measured in the SP phase, at 4 K, with $E \parallel$ chain. Bottom panel: The absorbance difference spectrum $\alpha_{4K} - \alpha_{16K}$ clearly shows an activated zone boundary mode at 284 cm^{-1} .

branches only at the Γ point ($k=0$), the softening can, strictly speaking, be investigated only by neutron scattering. Nevertheless, we tried to gain interesting insights from the temperature dependence of the phonon parameters obtained from the fit of the reflectivity data (see Fig. 10 and table I). In fact, if the dispersion and the mixing of the phonon branches are not too strong, one could hope that the presence of a soft mode at $k = (\pi/a, 0, \pi/c)$ would result in an overall softening of the branch it belongs to. Therefore, our first attempt was to check if any of the optical phonons detected in our experiments was showing a red shift upon cooling the sample. In Fig. 10 we can clearly observe that the B_{2u} mode ($E \perp$ chain) at 48 cm^{-1} is the only one showing an evident monotonic red shift from 300 to 15 K. Below T_{SP} this mode shows only a small blue shift. Also the behavior of the oscillator strength of this phonon is rather interesting: It grows continuously from 300 to 15 K (a $\sim 23\%$ increase), and it shows a sudden drop of $\sim 15\%$ across the phase transition. On the basis of these results, we could conclude that these particular phonon branch could have been a good candidate to show a real softening at the SP distortion vector in the Brillouin zone.

In order to check more directly the possible presence of a soft mode in CuGeO_3 , we performed transmission measurements with a mm-wave transmission setup, equipped with a backward wave oscillator operating in the frequency range $3.6\text{-}6.0 \text{ cm}^{-1}$.³⁵ The measurements were done on a $\sim 1 \text{ mm}$ thick sample of pure CuGeO_3 and, in order to relax the k -conservation rule and to obtain a result averaged over the all Brillouin zone, on Si and Mg substituted crystals, with approximately the same thickness of the pure one. In this way, we aimed to measure very accurately the transmission through the samples at one very low fixed frequency (5 cm^{-1}), as a function of temperature. If a mode would get soft, it would possibly

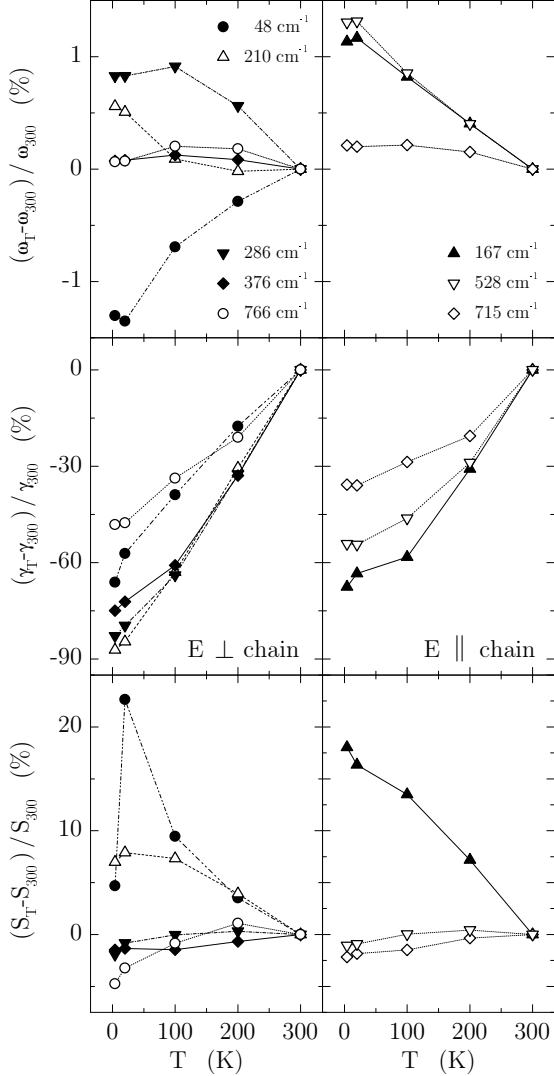


FIG. 10. Temperature dependence of the percentage change in resonant frequency, damping, and oscillator strength (from top to bottom) of the optical phonons of the undistorted phase, observed for $E \perp$ chain (left) and $E \parallel$ chain (right) on the pure single-crystal of CuGeO_3 .

result in a temperature dependent transmission showing a ‘w-shape’ centered at T_{SP} : Two minima in the absolute transmission, one on each side of T_{SP} . Unfortunately, we could not detect any change. Had we seen the expected ‘w-shape’ behavior, this would have been a strong indication of the existence of a soft mode in CuGeO_3 . In the present case we cannot confirm nor rule out a soft mode.

The final word about this issue had to come, as expected, from neutron scattering measurements. And indeed, recently, it was clearly shown that the pre-existing soft mode, expected in the classical theories of the SP phase transition,^{5,4} is not there in the case of CuGeO_3 .³⁶ Neither is present the central peak usually observed in order-disorder phase transitions.³⁰ In fact, Braden *et al.* investigated the lattice dynamics of CuGeO_3 with inelas-

Mode	Param.	4 K	15 K	100 K	200 K	300 K
B_{1u}	ω_{TO}	166.78	166.82	166.25	165.56	164.90
	γ	0.41	0.46	0.53	0.88	1.27
	S	0.348	0.343	0.335	0.316	0.295
B_{1u}	ω_{TO}	527.69	527.74	525.33	522.98	520.89
	γ	4.07	4.05	4.78	6.32	8.89
	S	1.900	1.903	1.921	1.929	1.921
B_{1u}	ω_{TO}	715.25	715.17	715.27	714.84	713.75
	γ	3.12	3.11	3.46	3.85	4.85
	S	0.636	0.638	0.640	0.648	0.650
B_{2u}	ω_{TO}	48.28	48.26	48.58	48.78	48.92
	γ	0.63	0.79	1.13	1.52	1.85
	S	0.286	0.335	0.299	0.282	0.273
B_{2u}	ω_{TO}	210.27	210.17	209.29	209.07	209.10
	γ	0.44	0.53	1.28	2.41	3.46
	S	1.717	1.732	1.723	1.669	1.605
B_{2u}	ω_{TO}	285.79	285.79	286.03	285.04	283.45
	γ	0.83	0.99	1.75	3.27	4.84
	S	0.765	0.773	0.780	0.782	0.780
B_{2u}	ω_{TO}	375.62	375.65	375.81	375.66	375.35
	γ	1.44	1.60	2.26	3.86	5.76
	S	0.596	0.597	0.596	0.601	0.605
B_{2u}	ω_{TO}	766.28	766.34	767.35	767.16	765.79
	γ	3.27	3.30	4.18	4.98	6.30
	S	0.677	0.689	0.705	0.718	0.711
$B_{1u, \text{SP}}$	ω_{TO}	284.21	-	-	-	-
	γ	—	-	-	-	-
	S	—	-	-	-	-
$B_{2u, \text{SP}}$	ω_{TO}	309.58	-	-	-	-
	γ	4.27	-	-	-	-
	S	0.003	-	-	-	-
$B_{2u, \text{SP}}$	ω_{TO}	799.75	-	-	-	-
	γ	2.32	-	-	-	-
	S	0.0007	-	-	-	-

TABLE I. Resonant frequency ω_{TO} (cm^{-1}), damping γ (cm^{-1}), and oscillator strength S of the optical phonons detected for $E \parallel$ chain (B_{1u} symmetry) and $E \perp$ chain (B_{2u} symmetry) on the pure single-crystal of CuGeO_3 . The parameters have been obtained by fitting the phonon spectra with Lorentz oscillators, at different temperatures.

tic neutron scattering combined with shell model lattice dynamical calculations.³⁶ They could identify the low-lying modes of the symmetry of the structural distortion characterizing the dimerized SP phase, and show that there is no soft mode behavior for these phonons at $k = (\pi/a, 0, \pi/c)$. Moreover, they found that the static SP distortion does not correspond to one single normal mode of the uniform phase, as usually expected for a continuous displacive transition,³⁰ but it corresponds to the linear combination, in ratio of 3:2, of two out of four optical phonons allowed by symmetry. Of these two modes, one involves an appreciable Cu displacement (essential for the dimerization), the second is associated with the twisting of the CuO_2 ribbons (which is the second element of the distortion). Finally, they showed that none of the two belongs to a branch having, at $k=0$, an opti-

cally allowed symmetry.³⁶

As a consequence of these findings, it appears that the behavior of the phonon parameters for the B_{2u} mode at 48 cm^{-1} is simply ‘accidental’. One may speculate that the absence of a softening at $k = (\pi/a, 0, \pi/c)$ implies that the phase transition is not driven by a softening of the phonon spectrum at $k = (\pi/a, 0, \pi/c)$, but only by a change in electronic structure which, in turn, determines the dynamical charge of the ions and the interatomic force constants. In this scenario, the large change in oscillator strength of some of the vibrational modes observed in our optical data (see Fig. 10), results from a change in ionicity, or, in other words, a transfer of spectral weight from the elastic degrees of freedom to electronic excitations. As far as the understanding of the SP phase transition in CuGeO_3 is concerned, now that the absence of a soft phonon is a well established experimental fact,³⁶ a further discussion will be presented in section VI.

A last remark has to be made regarding the temperature dependence of the B_{2u} mode observed at 286 cm^{-1} . On the basis of optical reflectivity measurements,³⁷ softening of this phonon, upon going through the phase transition, was suggested. This is not confirmed by our results which show no considerable frequency shift for this mode upon reducing the temperature from 15 to 4 K (see Fig. 10). On the other hand a reduction of both the scattering rate and the oscillator strength is observed, which can explain the double-peak structure in the reflectance ratio $R(20\text{ K})/R(5\text{ K})$ reported in Ref. 37.

C. Magnetic Excitations

Inelastic neutron and light scattering experiments are very sensitive to magnetic excitations and, in the case of CuGeO_3 , they have been very powerful tools in detecting the singlet-triplet magnetic gap,^{8,9} separated by a second gap from a continuum of magnon excitations,^{38–41} and a singlet bound-states within the two energy gaps.^{29,42} On the other hand, optical spectroscopy is usually not the elective technique to study this kind of processes, unless a static (charged magnons^{43,44}) or a dynamic (phonon assisted bi-magnons²⁷) breaking of symmetry is present in the system under investigation. Moreover, in these two latter cases, only those excitations characterized by a total $\Delta S = 0$ can be probed, because of spin conservation. Therefore, a direct singlet-triplet excitation is, in principle, not detectable. However, such a transition has been observed at 44.3 cm^{-1} in an infrared transmission experiment where the singlet-triplet nature of the transition was demonstrated by the Zeeman splitting observed applying a magnetic field.⁴⁵ In a later theoretical paper,⁴⁶ this line was interpreted as a magnetic excitation across the gap at the wave vector $(0, 2\pi/b, 0)$ in the Brillouin zone, activated by the existence of staggered magnetic fields along the direction perpendicular to the chains. Therefore, in a transmission experiment performed with

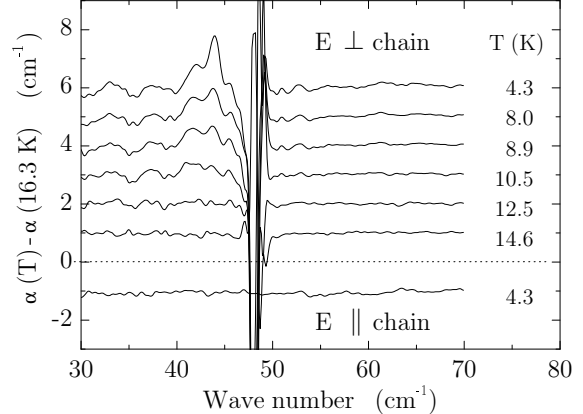


FIG. 11. Absorbance difference spectra for the pure single-crystal of CuGeO_3 , with $E \perp$ chain (top) and $E \parallel$ chain (bottom). The spectra have been shifted for clarity.

polarized light incoming onto the b - c plane of the sample at normal incidence, this excitation would be detectable only for magnetic field of the radiation parallel to the b axis of the crystal (\perp chain), i.e., E parallel to the c axis (\parallel chain).⁴⁶ In order to verify this interpretation, we measured the far-infrared transmission on a $350\text{ }\mu\text{m}$ thick pure single crystal of CuGeO_3 , for both $E \perp$ chain and $E \parallel$ chain. The absorbance difference spectra are reported in Fig. 11, where they have been shifted for clarity. Contrary to what expected following the interpretation given in Ref. 46, for $E \parallel$ chain (Fig. 11, bottom) no absorption is observed. However, for $E \perp$ chain (Fig. 11, top) an absorption peak, showing the temperature dependence appropriate for an excitation activated by the SP phase transition, is present at approximately 44 cm^{-1} . One has to note that the feature at 48 cm^{-1} is produced by the low-energy B_{2u} phonon. In fact, because of the complete absorption of the light in that frequency range, spikes are obtained when absorbance difference spectra are calculated. The observed polarization dependence puts a strong experimental constraint on the possible microscopic mechanism giving rise to the singlet-triplet absorption peak. For a complete understanding, a full experimental investigation of the symmetry of this magnetic absorption process by, e.g., measuring transmission through the a - b and a - c planes for different orientations of the electric and magnetic fields, is needed. A discussion of this feature, in relation to other critical theoretical and experimental aspects of the physics of CuGeO_3 , will be presented in section VI.

V. DOPED CuGeO_3

In this section we will present the optical spectroscopy data of several $\text{Cu}_{1-\delta}\text{Mg}_\delta\text{GeO}_3$ (with $\delta = 0, 0.01$), and $\text{CuGe}_{1-x}\text{B}_x\text{O}_3$ [with $B = \text{Si}$ ($x = 0, 0.007, 0.05, 0.1$), and Al ($x = 0, 0.01$)] single crystals. In particular, we investigated, as we did for the pure material, the phonon spec-

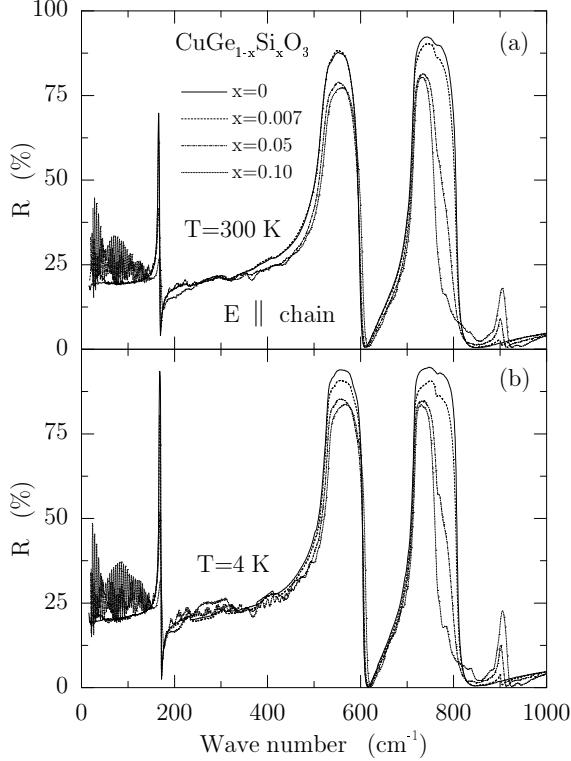


FIG. 12. c -axis reflectivity spectra of Si-doped single crystals of CuGeO_3 , for different silicon concentrations, at two different temperatures: $T=300$ K (a), and $T=4$ K (b).

trum as a function of temperature of Mg and Si substituted CuGeO_3 , by means of reflectivity measurements in the far-infrared region (see section V A). The aim of this investigation was, first of all, to study the effect of doping on the SP phase transition; second, to verify the recent claims of Yamada and co-workers^{47,48} who suggested that the structure originally proposed for CuGeO_3 , in the high temperature undistorted phase,² could be wrong (see section V A). Moreover, transmission measurements in the mid-infrared region were performed on all the samples, in order to detect possible electronic and/or magnetic excitation which could provide us with additional information about the interplay of spin and charge in this quasi-1D systems (see section V B).

A. Far-Infrared Reflection

The reflectivity data acquired on the Si doped samples for $E \parallel \text{chain}$ (c axis), and $E \perp \text{chain}$ (b axis), are shown in Fig. 12 and 13, respectively. The spectra are similar to those we already discussed for pure CuGeO_3 . However, some new features, stronger in intensity the higher the Si concentration, are observable already at room temperature. Therefore, they are due to the substitution of Ge with the lighter Si and not directly related to the SP transition: New phonon peaks at 900 cm^{-1} , along the

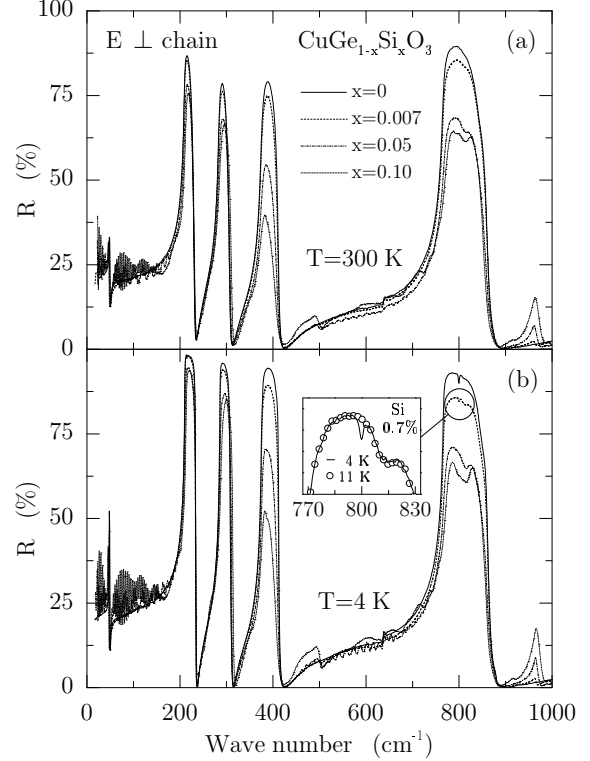


FIG. 13. b -axis reflectivity spectra of Si-doped single crystals of CuGeO_3 , for different silicon concentrations, at two different temperatures: $T=300$ K (a), and $T=4$ K (b). The 800 cm^{-1} folded mode, activated by the SP transition, is still observable for 0.7% Si-doping by comparing (see inset) the 4 K (solid line) and the 11 K (circles) data.

c axis (Fig. 12), and at 500 and 960 cm^{-1} , along the b axis (Fig. 13). Moreover, the much more complicated line shape and the considerable reduction of the oscillator strength of the high frequency phonons indicate: First, a strong Ge (Si) contribution to these modes, mainly due to O vibrations.²⁰ Second, that substituting Si for Ge has apparently a strong symmetry-lowering effect, a point which we will discuss again later in relation to the claim of Yamada *et al.*^{47,48} about a possible lower symmetry, with respect to the one originally proposed by Völlenkne *et al.*,² for the uniform structure of CuGeO_3 . At temperatures lower than T_{SP} (Fig. 13b), we can observe the folded mode at 800 cm^{-1} along the b axis, previously detected on pure CuGeO_3 (see section V A). However, it is found only for the lowest Si concentration, as shown in the inset of Fig. 13b, where the 4 K and 11 K data are compared. We can conclude that up to 0.7% Si doping the SP transition is still present with $T_{\text{SP}} < 11$ K, whereas for 5% and 10% Si concentrations no signature of the transition could be found in our spectra.

The results obtained on the 1% Mg-doped sample are plotted, together with the results obtained on pure CuGeO_3 , in Fig. 14 and Fig. 15 for $E \parallel \text{chain}$ (c axis), and $E \perp \text{chain}$ (b axis), respectively. Clearly, Mg doping

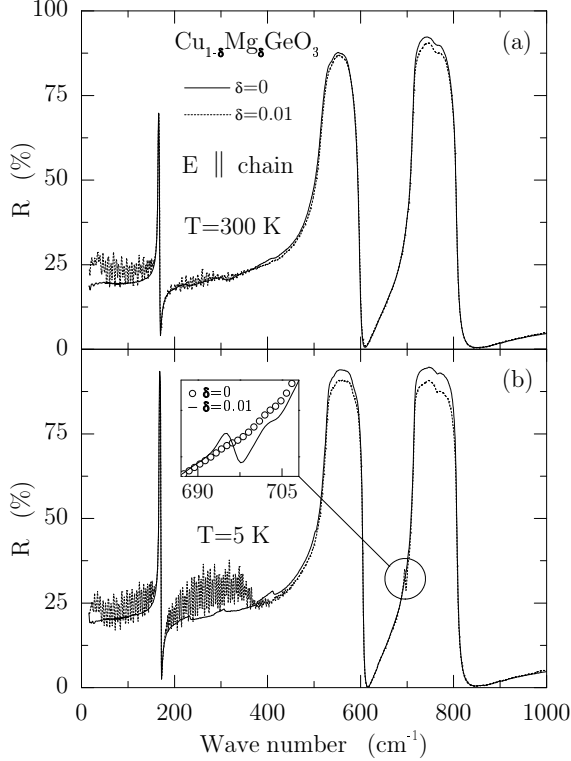


FIG. 14. c -axis reflectivity spectra of pure and 1% Mg-doped single crystals of CuGeO_3 , at two different temperatures: $T=300$ K (a) and $T=5$ K (b). The inset shows an enlarged view of the frequency region around 700 cm^{-1} for the data obtained on the pure (circles) and Mg-doped (solid line) samples, at $T=5$ K. The additional peak observed for Mg doping is due to the mass difference between Cu and Mg and it is not related to the SP transition.

is affecting the optical response of CuGeO_3 less than Si doping does. A new phonon, due to the mass difference between Cu and Mg, is present in the c -axis spectra at 695 cm^{-1} , as clearly shown in the inset of Fig. 14b, for $T=5$ K. Moreover, we clearly observe for $E \perp$ chain (see inset of Fig. 15b), the 800 cm^{-1} zone boundary mode activated by the SP transition. On the one hand, for the 1% Mg-doped sample, T_{SP} seems to be lower than in pure CuGeO_3 ; on the other hand, the structural deformation is not as strongly reduced as in the 0.7% Si-doped sample, as can be deduced from the direct comparison between the insets of Fig. 13b and Fig. 15b.

In order to estimate more precisely the reduction the oscillator strength for the 800 cm^{-1} phonon, and eventually the decrease of T_{SP} with respect to what was observed on pure CuGeO_3 , we made careful measurements for $T < T_{\text{SP}}$ on the 1% Mg and the 0.7% Si-doped samples (see Fig. 16 and 17, respectively). In both cases we can observe, in the reflectivity spectra, the gradual disappearance of the activated phonon for $T \rightarrow T_{\text{SP}}$ from below and, in the optical conductivity (see insets of Fig. 16 and 17), the additional peak present in the dimerized phase data, superimposed to the background of the B_{2u}

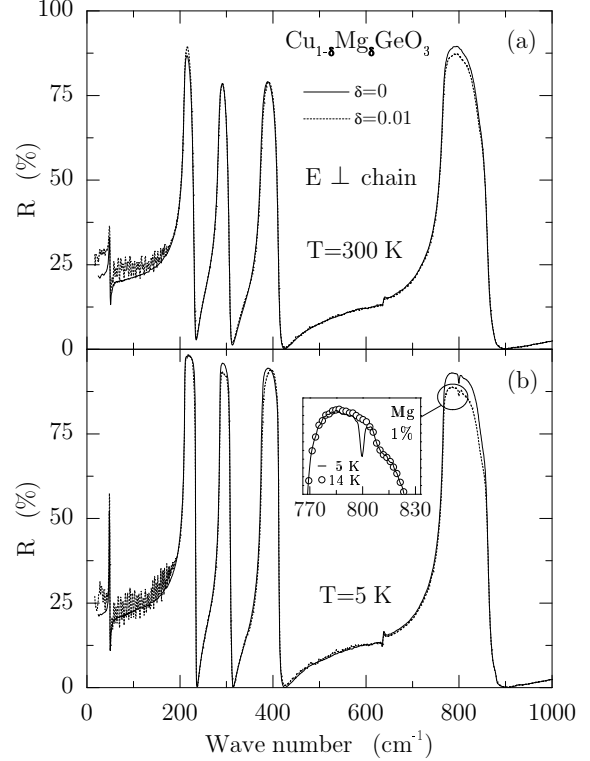


FIG. 15. b -axis reflectivity spectra of pure and 1% Mg-doped single crystals of CuGeO_3 , at two different temperatures: $T=300$ K (a) and $T=5$ K (b). For the Mg-doped sample the 800 cm^{-1} folded mode, activated by the SP transition, is clearly observable in the inset where the 5 K (solid line) and the 14 K (circles) data are presented.

phonon of the high symmetry phase. As for the pure material (section IV A), by fitting the reflectivity spectra with Lorentz oscillators for the optical phonons, we could obtain the temperature dependence of the oscillator strength for the 800 cm^{-1} line. The results are plotted for all the samples in Fig. 18. For pure CuGeO_3 we saw that our results for the oscillator strength of the activated optical phonon are in very good agreement with the peak intensity of a superlattice reflection measured by Harris *et al.*²⁶ (see Fig. 18). Similarly, the data obtained on doped samples, compare nicely to those presented, for 0.7% Si doping, in Ref. 49 and, for 1% Mg doping, to those reported in Ref. 50 for an 0.9% Zn-doped sample (superlattice reflection data for Mg-doped CuGeO_3 , obtained by neutron-scattering, became available in the literature only very recently,⁵¹ however for a too high Mg concentration to be directly comparable to our results).

It is not possible to perform the same fit for the data acquired on doped samples, as we did on the pure crystal, because they are characterized by an upturned curvature near T_{SP} , which can be explained in terms of a distribution of transition temperatures due to the disorder introduced upon doping the system.⁴⁹ However, for the 1% Mg and the 0.7% Si doped samples the estimates

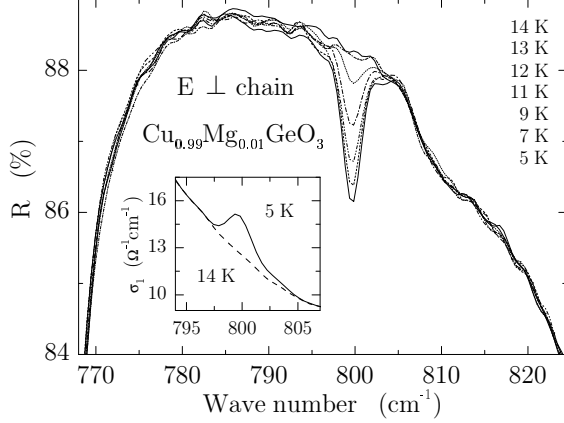


FIG. 16. Detailed temperature dependence of the 800 cm^{-1} activated mode observed with $E \perp$ chain in the reflectivity spectra of $\text{Cu}_{0.99}\text{Mg}_{0.01}\text{GeO}_3$, for $T < T_{\text{SP}}$. In the inset, where the dynamical conductivity calculated via Kramers-Kronig analysis is plotted, a new peak is clearly visible for $T = 5 \text{ K}$.

for T_{SP} of approximately 12.4 K and 9.3 K , respectively, can be obtained (Fig. 18). Considering that usually, for pure CuGeO_3 , $T_{\text{SP}} \approx 14.2$ (on our pure sample a slightly reduced value has been observed), we can conclude that Si is three times more effective in reducing T_{SP} than Mg. This result has recently been confirmed, on a more strong basis, by a very systematic and detailed investigation of the decrease of T_{SP} and of the occurrence of 3D AF order at lower temperature on several doped single crystals of CuGeO_3 , by magnetic susceptibility measurements.⁵²

The difference between Mg and Si in influencing the phase transition can be understood considering what is the effect of these two different ways of doping on the magnetism of the system. The substitution of a Cu^{2+} ion by a non magnetic impurity, like Mg, effectively cuts the CuO_2 chain in two segments and, at the same time, breaks a singlet dimer. Therefore, a free $S=1/2$ Cu^{2+} spin is created for each Mg impurity. More subtle is the effect of the substitution of Ge with Si: As shown by Khomskii and co-workers,^{53,54} it has to do with the question why the Cu-Cu nn superexchange interaction in CuGeO_3 is AF in the first place. In fact, because the Cu-O(2)-Cu bond angle is $\gamma \approx 98^\circ$, and because the Goodenough-Kanamory-Anderson rule⁵⁵ states that the 90° superexchange of two magnetic ions (via a ligand), with partially filled d shells, is (weakly) ferromagnetic, it is not that obvious why the nn superexchange is AF in CuGeO_3 . Khomskii and co-workers^{53,54} calculated that the 8° deviation from the critical value of 90° is not sufficient for the superexchange to change sign. The AF interaction was shown to be a consequence of the side-group effect. In fact, because of the presence of Ge and, in particular, because of the Ge-O hybridization, the oxygen p_x and p_y orbitals are not equivalent any more. Therefore, the cancellation of the AF contributions to the Cu-Cu superexchange, via the ligand O, is no longer complete,

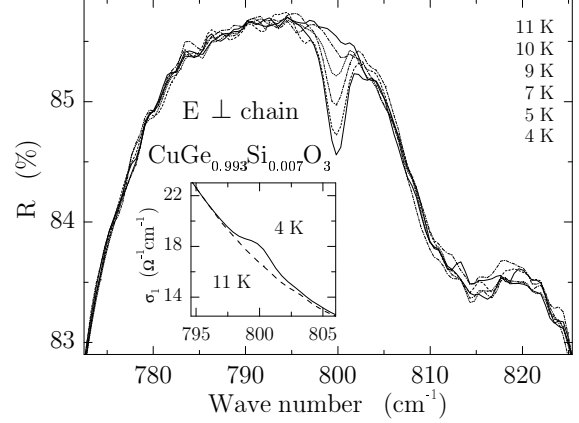


FIG. 17. Detailed temperature dependence of the 800 cm^{-1} activated mode observed with $E \perp$ chain in the reflectivity spectra of $\text{CuGe}_{0.993}\text{Si}_{0.007}\text{O}_3$, for $T < T_{\text{SP}}$. In the inset, where the dynamical conductivity calculated via Kramers-Kronig analysis is plotted, a new peak is clearly visible for $T = 4 \text{ K}$.

resulting in a (weak) AF superexchange. When Ge is substituted with Si, one could at first glance expect a relatively weak effect because, contrary to the substitution of Cu with Mg, Si is not directly breaking a dimer. However, because Si is smaller than Ge, both the Si-O bond length [which is proportional the Cu-O(2)-Cu bond angle γ] and the Si-O hybridization are reduced.^{53,54} As a result, Si breaks the Cu-Cu superexchange interaction on the two neighboring CuO_2 chains adjacent to the Si^{4+} ion. This explains, at least qualitatively, why Si has to be much more efficient than Mg in reducing T_{SP} .

Recently Yamada and co-workers^{47,48} raised doubts about the structure of CuGeO_3 in the high-temperature undistorted phase. They showed that the results of electron paramagnetic resonance experiments⁴⁷ can be fully understood only taking into account spin-antisymmetric interaction, such as the Dzyaloshinsky-Moriya exchange interaction.⁵⁶ However, the antisymmetric exchange interaction is strictly forbidden in the space group $Pbmm$ because the midpoint in between two adjacent Cu^{2+} ions, along the CuO_2 chains, has inversion symmetry. To verify these findings, x-ray diffraction experiments were performed by Hidaka *et al.*,⁴⁸ at room temperature, on pure single crystals grown by the floating-zone method, subsequently improved in their quality by a combined annealing and slow cooling process. As a result, new superlattice reflections were found, related to tilting and rotation of the GeO_4 tetrahedra in four different manners along the c axis, and in antiphase along the a axis. As a consequence, local distortions of the CuO_6 octahedra are induced, with a four times periodicity along the c axis. The space group was determined to be $P2_12_12_1$, with an eight times larger unit cell, i.e., $2a \times b \times 4c$, with respect to the one originally proposed by Völlenkle *et al.*² According to Hidaka *et al.*,⁴⁸ this additional deformation of the structure would be there also on non carefully

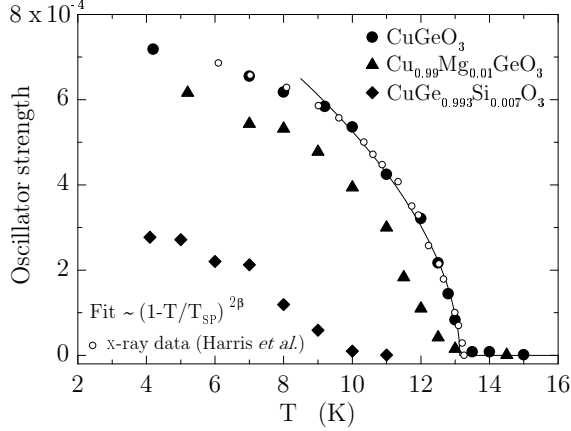


FIG. 18. Temperature dependence of the oscillator strength of the zone boundary folded mode observed, for $E \perp$ chain, at 800 cm^{-1} on pure, 1% Mg-doped, and 0.7% Si-doped CuGeO_3 single crystals. The x-ray scattering data of Harris *et al.*²⁶ and the fit to the power law described in section IV A are also plotted, for pure CuGeO_3 .

annealed single crystals, but only on a short-range scale. Moreover, the newly proposed structure allows for the antisymmetric exchange interaction which was required to interpret the electron paramagnetic resonance results⁴⁷ on both annealed and as-grown samples, because the Dzyaloshinsky-Moriya exchange interaction depends only on the local symmetry around the nn spins.⁵⁶

This could have strong consequences for the picture of the SP transition in CuGeO_3 , because it implies the presence of four different values of the superexchange interaction at room temperature and, upon decreasing the temperature toward T_{SP} , strong fluctuations of the exchange interactions, induced by the increasing lattice instability. As the $P2_12_12_1$ group has fewer symmetry elements than the conventional $Pbmm$, a larger number of phonon modes should be observed in the optical spectra. Skipping the details of the calculation, the irreducible representations of the optical vibrations of CuGeO_3 in the high temperature phase, for the space group $P2_12_12_1$, is:

$$\Gamma'' = 56A(aa, bb, cc) + 55B_1(ab; E||c) + 63B_2(ac; E||b) + 63B_3(bc; E||a), \quad (5)$$

corresponding to 63, 63, and 55 optical active modes along the a , b , and c axes, respectively. As we already discuss in section IV A, the number of phonons detected in the reflectivity spectrum of pure CuGeO_3 was in agreement with the results of the group theoretical analysis for the space group $Pbmm$ proposed by Völlenklee *et al.*² At the same time, as observed by Yamada and co-workers,^{47,48} the additional distortion, characterizing the $P2_12_12_1$ space group, is present only on a short-range scale in as-grown samples, like the ones used in this experimental work. However, even on pure CuGeO_3 , in fitting the reflectivity spectra with Lorentz oscillators for the optical phonons, we had to add, in order to be able

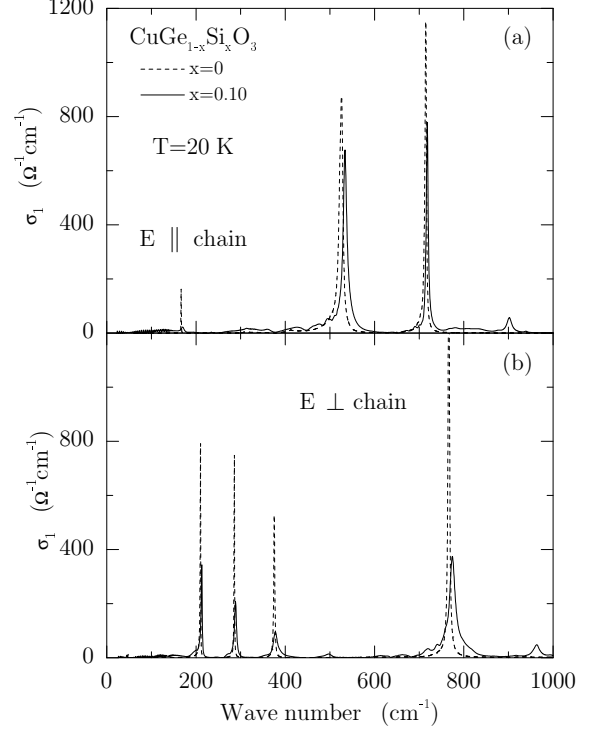


FIG. 19. Low temperature optical conductivity spectra, obtained by Kramers-Kronig analysis, of pure and 10% Si-doped CuGeO_3 , for $E \parallel$ chain (a) and $E \perp$ chain (b). Note that in panel (b) the data on pure CuGeO_3 have been clipped in order to use the same scale as in panel (a): in fact, the peak value of the phonon at 766 cm^{-1} is $2010 \text{ } \Omega^{-1} \text{ cm}^{-1}$.

to exactly reproduce the experimental data, a number of very weak and broad additional peaks, of unclear origin. In this context, the results obtained on Si substituted CuGeO_3 single crystals seem to be more significant. We already mentioned how strongly the phonon spectra were affected by the presence of Si in the samples. This effect is even more evident when the optical conductivity spectra are considered. In Fig. 19, the low temperature optical conductivity of pure and 10% Si-doped CuGeO_3 , for $E \parallel$ chain (a) and $E \perp$ chain (b), is plotted. We can observe a reduction of oscillator strength and a broadening for all the lattice vibrations. Moreover, additional bands appear over the all range, as clearly shown in Fig. 20, where the low temperature optical conductivity, for all the measured Si-doped samples, is presented. We can see that not only sharp peaks appear at 900 and 960 cm^{-1} along the c and b axes, respectively, as discussed at the beginning of this section. There is also a large number of phonon bands, growing in intensity upon increasing the Si concentration, at both low and high frequencies. It is obviously not possible to check in detail whether we detected all the modes expected, on the basis of group theory, for the newly proposed space group $P2_12_12_1$.^{47,48} There are simply too many of them, in both theory (see Eq. 5) and experiment (see Fig. 20). Moreover, we have to take into account that, in general, the introduction

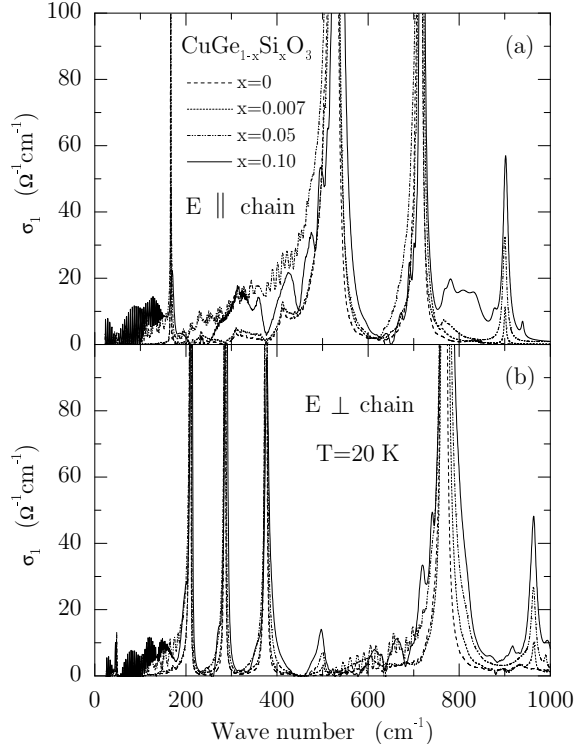


FIG. 20. Low temperature optical conductivity, obtained by Kramers-Kronig analysis, of pure and several Si-doped CuGeO_3 single crystals, for $E \parallel$ chain (a) and $E \perp$ chain (b).

of impurities in a crystal results in a relaxation of the k conservation rule. Therefore, states with $k \neq 0$ are projected back to the Γ point, and phonon bands averaged over the entire Brillouin zone can be measured in an optical experiment. However, we may speculate that Si, that has such a strong influence on T_{SP} via the side group effect,^{53,54} could also be responsible for enhancing the underlying lattice distortion which was suggested to be already present in pure CuGeO_3 , by Yamada and co-workers.^{47,48} In our opinion these results, although not conclusive, indicate that a symmetry lower than the one assumed until now could be possible. In particular, it should be taken into account as one of the possible explanations for the aspects still unresolved of the physics of CuGeO_3 (see section VI).

B. Mid-Infrared Transmission

In this section we will discuss the optical data obtained by performing transmission experiments, in the range going from 400 to 8000 cm^{-1} , on several $\text{Cu}_{1-\delta}\text{Mg}_\delta\text{GeO}_3$ (with $\delta=0, 0.01$), and $\text{CuGe}_{1-x}\text{B}_x\text{O}_3$ [with $B=\text{Si}$ ($x=0, 0.007, 0.05, 0.1$), and Al ($x=0, 0.01$)] single crystals. In particular, by combining reflectivity and transmission results, we could calculate the optical conductivity by direct inversion of the Fresnel formula.²² By this investigation, we aimed to study

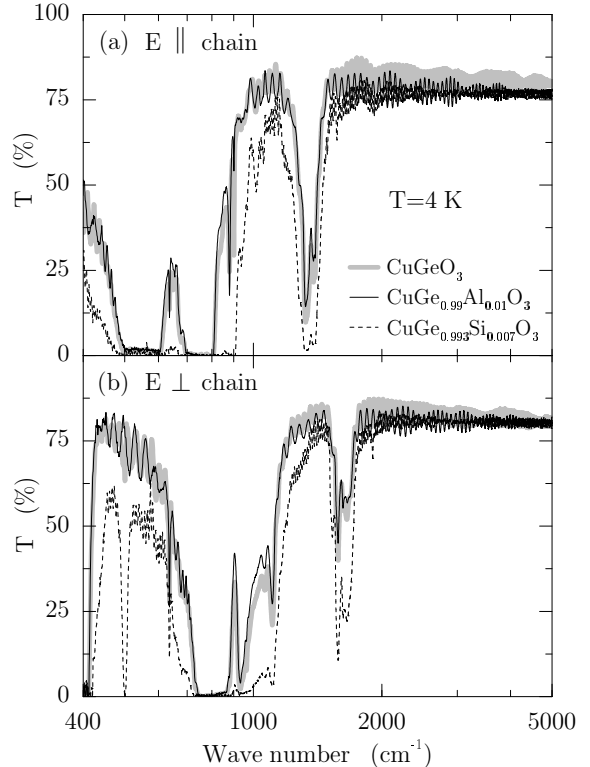


FIG. 21. Low temperature transmission spectra of pure, 1% Al, and 0.7% Si doped CuGeO_3 , for $E \parallel$ chain (a) and $E \perp$ chain (b).

whether, in CuGeO_3 , doping has an effect on the electronic and/or magnetic excitations similar to what has been observed on the underdoped parent compounds of high- T_c superconductors.^{57–59} In fact, on the latter materials, chemical substitution introduces charge carriers in the 2D Cu-O planes, resulting in a disappearance of the gap and in the transfer of spectral weight into a Drude peak, for the in-plane optical response. Moreover, the so called ‘mid-infrared’ band, whose interpretation is still controversial, is usually present in these systems.^{57–59}

The low temperature (4 K) transmission spectra of pure, 1% Al, and 0.7% Si doped CuGeO_3 , for $E \parallel$ chain and $E \perp$ chain, are plotted in Fig. 21a and 21b, respectively. Spectra at different temperatures above and below the phase transition were measured. However, the results are not shown because no particular temperature dependence was observed in cooling down the sample from room temperature to T_{SP} , nor across the phase transition. Similarly, the spectra for 1% Mg and 5 and 10% Si doped crystals are not presented because no additional information can be obtained from these results. As shown by Fig. 21, the transmission through pure CuGeO_3 , in this frequency region, is mainly characterized by the strong absorptions of the phonons of the high symmetry phase at 528 and 715 cm^{-1} , along the c axis, and at 376 and 766 cm^{-1} , along the b axis. In addition, many multiphonon bands are present, the most intense ones being at

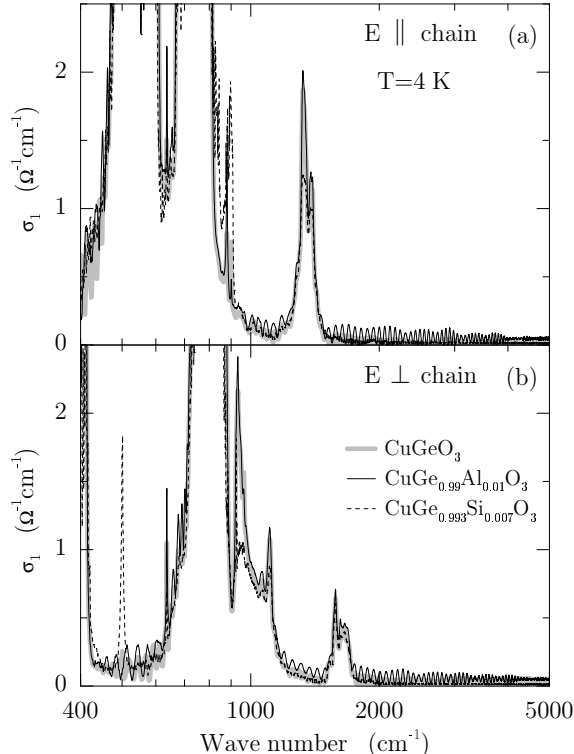


FIG. 22. Low temperature conductivity spectra, obtained by direct inversion of the Fresnel formula, of pure, 1% Al, and 0.7% Si doped CuGeO_3 , for $E \parallel \text{chain}$ (a) and $E \perp \text{chain}$ (b). Note the very low value of $\sigma_1(\omega)$.

1330 and 1580 cm^{-1} along the c and b axes, respectively. The same features are observable on the doped samples where, however, more multiphonon bands are detected reflecting the presence of additional peaks in the single-phonon spectrum, already discussed in section V A on the basis of reflectivity measurements. A last remark has to be made about the oscillations present in all the spectra of Fig. 21. These are, as mentioned before, interference fringes due to Fabry-Perot resonances;²² the different period of the interference pattern for the three crystals is simply due to the different thickness of the samples used in the experiments.

If we now consider the optical conductivity spectra plotted in Fig. 22, it is clear that nothing else has been detected, in this frequency range, besides absorption processes purely related to lattice degrees of freedom. In particular, for all the samples, the conductivity is just zero from 2000 to 8000 cm^{-1} . From these results and from the fact that no signature of a Drude peak was observed in any of the doped samples in reflectivity experiments (see section V A), we conclude that no charge carriers are introduced in the CuGeO_3 by the different chemical substitutions we tried, nor magnetic/dielectric polarons (observed, e.g., in ultra low doped $\text{YBa}_2\text{Cu}_3\text{O}_6$ ^{58,59}). One has to note that, in this sense, the most significant of the results we showed is the one obtained on Al substituted CuGeO_3 because in this case, contrary to Si substitution,

Ge is replaced by an element with different valence.

VI. DISCUSSION

As shown in the course of this paper, in our investigation of pure and doped CuGeO_3 with optical spectroscopy, we observed features which are not completely understandable on the basis of Cross and Fisher theory for the SP phase transition,⁴ and of the achieved picture of the SP transition in CuGeO_3 . No pre-existing soft mode was detected, not only in our optical measurements, but especially in neutron scattering experiments.³⁶ This result could explain why the value of β in the expression describing the temperature dependence of the order parameter close to T_{SP} [$\delta \sim (1 - T/T_{\text{SP}})^\beta$] deviates, in CuGeO_3 , from the mean-field behavior $\beta = 1/4$ observed in the TTF salt (see section IV A). Moreover, a direct singlet-triplet excitation across the magnetic gap, possibly at the wave vector $(0, 2\pi/b, 0)$ in the Brillouin zone, was detected in our transmission spectra. This excitation is, in principle, ‘doubly’ forbidden: In fact, because of symmetry considerations and of spin conservation we are restricted, in an optical experiment, to excitations characterized by $k = 0$ and $\Delta S = 0$. Finally, strong changes in the phonon spectrum were observed on Si-substituted samples, which might be explained in terms of the alternative space group $P2_12_12_1$, recently proposed for CuGeO_3 in the high temperature uniform phase.^{47,48}

Many attempts have recently been made to improve the understanding of the SP phase transition in CuGeO_3 . In particular, it has been shown that the adiabatic treatment of the 3D phonon system, characteristic for the Cross and Fisher theory,⁴ is not appropriate for the case of CuGeO_3 , where the phonons contributing appreciably to the SP distortion have energies much higher than the magnetic gap.^{60,61} An alternative description of the SP transition, not based on the assumption of phononic adiabaticity, was developed by Uhrig:⁶⁰ Phonons are considered as the fast subsystem, responsible for the interchain coupling, and an effective dressed spin model is derived. As a result, the soft phonon is absent and the SP transition is characterized by growing domains of coherent dimerization, whose size diverges at T_{SP} . Alternatively, Gros *et al.*⁶¹ showed that no inconsistency is present in Cross and Fisher theory:⁴ They concluded that, in Cross and Fisher framework, a soft phonon has to be present only if the bare phonon frequency satisfies the relation $\Omega_0 < 2.2 T_{\text{SP}}$. For larger phonon frequencies only a central peak is expected at T_{SP} . However, this new collective excitation, which would consist of the linear superposition of a phonon with two magnons in a singlet state,⁶¹ has not been observed up to now. Moreover, it has been shown that for a detailed understanding of magnetic susceptibility^{1,10} and magnetostriction^{62,63} data and, at the same time, of the singlet and triplet

excitation branches below the continuum,^{29,38} not only the 2D character of the system cannot be neglected,^{8,60} but also both the nn (J_1) and the nnn (J_2) magnetic exchange interactions have to be taken into account in CuGeO₃.^{63–65} The system would then be described by an alternating and frustrated AF 1D Heisenberg spin-chain model:

$$H = J \sum_j \left\{ [1 + \delta(-1)^i] \vec{S}_j \cdot \vec{S}_{j+1} + \alpha \vec{S}_j \cdot \vec{S}_{j+2} \right\}, \quad (6)$$

where δ is the static dimerization parameter and $\alpha = J_1/J_2$ is the frustration parameter. In particular, the value $\alpha = 0.354$ was obtained,^{63–65} which is significantly larger than the critical value sufficient for the formation of a spontaneous gap in the magnetic excitation spectrum, in absence of lattice dimerization, i.e., $\alpha_c = 0.241$.^{66,67} However, on the basis of this approach and, in particular, with the large value obtained for α , the amplitude of the dimerization δ , estimated by reproducing the singlet-triplet excitation gap,^{68,69} is substantially underestimated. In fact in this way, the very small value $\delta \simeq 0.012$ is obtained, whereas, from the combined analysis of the structural lattice distortion in the dimerized phase and of the magneto-elastic coupling in the uniform phase (from magnetostriction measurements), the value $\delta \simeq 0.04–0.05$ results.⁷⁰ Still retaining the value $\alpha = 0.354$, a consistent value for the lattice dimerization (i.e., of the order of 5%) is obtained from the analysis of the inelastic neutron scattering data if, instead of a static dimerization parameter δ , an explicit coupling between the spins and the three dimensional phonon system is introduced in the Hamiltonian given in Eq. 6.⁷¹

In relation to the space group $P2_12_12_1$, recently proposed for CuGeO₃ in the high temperature phase,^{47,48} besides the optical data on Si-substituted samples we presented, very interesting are the inelastic neutron scattering results reported by Lorenzo *et al.*⁷² A second singlet-triplet (optical) branch was observed in pure CuGeO₃, with a gap value at the Γ point of ~ 5.8 meV. The dispersion of this newly found optical mode is identical to the one of the acoustic mode, but shifted by $(2\pi/b + \pi/c)$. Lorenzo *et al.*⁷² proposed that the origin of this second mode is the relative orientation of the Cu-O(2)-Cu units between next neighboring chains along the b axis, along with a small spin-orbit coupling. This would give rise the slight distortion of the spin isotropy necessary to reproduce the finite intensity for the optical triplet mode and the difference in the scattering intensities between the optical and the acoustic branches.⁷² On the other hand, anisotropy in the magnetic exchange constants along the b axis, below T_{SP} , ought to be present in the space group $P2_12_12_1$ proposed by Yamada *et al.*,^{47,48} because of the strong fluctuations of the exchange interactions expected upon decreasing the temperature toward T_{SP} .

These results are not only showing that the structure generally assumed for CuGeO₃ in the uniform phase may be incorrect, but they are also suggesting a possible explanation for the singlet-triplet excitation we observed in

transmission at ~ 44 cm⁻¹ ~ 5.5 meV. In fact, such an optical transition, with approximately the right energy value, is now present at $k=0$ and not only at the wave vector $(0, 2\pi/b, 0)$, which is not accessible in an optical experiment. The final constraint $\Delta S = 0$ which is not satisfied for this excitation, could be possibly explained as a consequence of spin-orbit interaction, which relaxes the spin conservation rule. In order to assess whether this absorption line is given to an electric dipole or to a magnetic dipole transition, in presence of spin-orbit interaction, a careful analysis of selection rules and absolute intensities is needed.

VII. CONCLUSIONS

In this paper we have been discussing in detail the temperature dependent optical response of pure and doped CuGeO₃, in the frequency range going from 20 to 32 000 cm⁻¹, with particular emphasis on the infrared phonon spectra. We could detect zone boundary folded modes activated by the SP phase transition. Following the temperature dependence of these modes we were able to determine the second order character of the phase transition and to study the effect of doping on T_{SP} : In particular, we showed that the substitution of Ge with Si is three times more efficient, than the one of Cu with Mg, in reducing T_{SP} . This was explained, following Khomskii and co-workers,^{53,54} as a consequence of the side-group effect.

Moreover, in transmission experiments we detected a direct singlet-triplet excitation, across the magnetic gap, which is not understandable on the basis of the magnetic excitation spectrum generally assumed for CuGeO₃. The optical activity of this excitation has been discussed in relation to newly reported inelastic neutron scattering data which show the existence of a second (optical) magnetic branch.⁷² The anisotropy in the magnetic exchange constants along the b axis, necessary for the optical triplet mode in order to gain a finite intensity, and the strong changes in the phonon spectra of Si-substituted samples might be explained in terms of the alternative space group $P2_12_12_1$, recently proposed for CuGeO₃ in the high temperature uniform phase.^{47,48}

VIII. ACKNOWLEDGEMENTS

We gratefully acknowledge M. Mostovoy and D.I. Khomskii for stimulating discussions, and P.H.M. van Loosdrecht, J.E. Lorenzo, and M. Grüninger for many useful comments. One of us (A.D.) is pleased to thank M. Picchietto and B. Topić for assistance. This investigation was supported by the Netherlands Foundation for Fundamental Research on Matter (FOM) with financial aid from the Nederlandse Organisatie voor Wetenschappelijk Onderzoek (NWO).

* Present address: Center for Materials Research, McCullough Building, Stanford University, 476 Lomita Mall, Stanford, CA 94305-4045. E-mail: damascel@stanford.edu

- ¹ M. Hase, I. Terasaki, and K. Uchinokura, Phys. Rev. Lett. **70**, 3651 (1993).
- ² H. Völlenkne, A. Wittmann, and H. Nowotny, Monatsh. Chem. **98**, 1352 (1967).
- ³ E. Pytte, Phys. Rev. B **10**, 4637 (1974).
- ⁴ M.C. Cross, and D.S. Fisher, Phys. Rev. B **19**, 402 (1979).
- ⁵ L.N. Bulaevskii, A.I. Buzdin, and D.I. Khomskii, Solid State Commun. **27**, 5 (1978).
- ⁶ M.C. Cross, Phys. Rev. B **20**, 4606 (1979).
- ⁷ For a review, see J.P. Boucher, and L.P. Regnault, J. Phys. I **6**, 1939 (1996).
- ⁸ M. Nishi, O. Fujita, and J. Akimitsu, Phys. Rev. B **50**, 6508 (1994).
- ⁹ O. Fujita, J. Akimitsu, M. Nishi, and K. Kakurai, Phys. Rev. Lett. **74**, 1677 (1995).
- ¹⁰ J.P. Pouget, L.P. Regnault, M. Aïn, B. Hennion, J.-P. Renard, P. Veillet, G. Dhalenne, and A. Revcolevschi, Phys. Rev. Lett. **72**, 4037 (1994).
- ¹¹ K. Hirota, D.E. Cox, J.E. Lorenzo, G. Shirane, J.M. Tranquada, M. Hase, K. Uchinokura, H. Kojima, Y. Shibuya and I. Tanaka, Phys. Rev. Lett. **73**, 736 (1994).
- ¹² M. Braden, G. Wilkendorf, J. Lorenzana, M. Aïn, G.J. McIntyre, M. Behruzi, G. Heger, G. Dhalenne, and A. Revcolevschi, Phys. Rev. B **54**, 1105 (1996).
- ¹³ M. Hase, I. Terasaki, K. Uchinokura, M. Tokunaga, N. Miura, and H. Obara, Phys. Rev. B **48**, 9616 (1993).
- ¹⁴ T. Lorenz, U. Ammerahl, T. Auweiler, B. Büchner, A. Revcolevschi, and G. Dhalenne, Phys. Rev. B **55**, 5914 (1997).
- ¹⁵ J.W. Bray, H.R. Hart, L.V. Interrante, I.S. Jacobs, J.S. Kasper, G.D. Watkins, and S.H. Wee, Phys. Rev. Lett. **35**, 744 (1975).
- ¹⁶ I.S. Jacobs, J.W. Bray, H.R. Hart, L.V. Interrante, J.S. Kasper, G.D. Watkins, D.E. Prober, and J.C. Bonner, Phys. Rev. B **14**, 3036 (1976).
- ¹⁷ S. Huizinga, J. Kommandeur, G.A. Sawatzky, B.T. Thole, K. Kopinga, W.J.M. de Jonge, and J. Roos, Phys. Rev. B **19**, 4723 (1979).
- ¹⁸ A. Damascelli, D. van der Marel, F. Parmigiani, G. Dhalenne, and A. Revcolevschi, Physica B **244**, 114 (1998).
- ¹⁹ D.L. Rousseau, R.P. Bauman, and S.P.S. Porto, J. Raman Spectrosc. **10**, 253 (1981).
- ²⁰ Z.V. Popović, S.D. Dević, V.N. Popov, G. Dhalenne, and A. Revcolevschi, Phys. Rev. B **52**, 4185 (1995).
- ²¹ A. Revcolevschi, and G. Dhalenne, Adv. Mater. **5**, 657 (1993).
- ²² M.V. Klein, and T.E. Furtak, *Optics* (John Wiley & Sons, New York, 1983).
- ²³ I. Terasaki, R. Itti, N. Koshizuka, M. Hase, I. Tsukada, and K. Uchinokura, Phys. Rev. B **52**, 295 (1995).
- ²⁴ M. Bassi, P. Camagni, R. Rolli, G. Samoggia, F. Parmigiani, G. Dhalenne, and A. Revcolevschi, Phys. Rev. B

- 54**, R11 030 (1996).
- ²⁵ A. Damascelli, D. van der Marel, F. Parmigiani, G. Dhalenne, and A. Revcolevschi, Phys. Rev. B **56**, R11 373 (1997).
- ²⁶ Q.J. Harris, Q. Feng, R.J. Birgeneau, K. Hirota, G. Shirane, M. Hase, and K. Uchinokura, Phys. Rev. B **52**, 15 420 (1995).
- ²⁷ J. Lorenzana, and G.A. Sawatzky, Phys. Rev. Lett. **74**, 1867 (1995).
- ²⁸ Q.J. Harris, Q. Feng, R.J. Birgeneau, K. Hirota, K. Kakurai, J.E. Lorenzo, G. Shirane, M. Hase, K. Uchinokura, H. Kojima, I. Tanaka, and Y. Shibuya, Phys. Rev. B **50**, 12 606 (1994).
- ²⁹ G. Els, P.H.M. van Loosdrecht, P. Lemmens, H. Vonberg, G. Güntherodt, G.S. Uhrig, O. Fujita, J. Akimitsu, G. Dhalenne, and A. Revcolevschi, Phys. Rev. Lett. **79**, 5138 (1997).
- ³⁰ A.D. Bruce, and R.A. Cowley, *Structural Phase Transitions* (Taylor & Francis, London, 1981).
- ³¹ M.D. Lumsden, B.D. Gaulin, and H. Dabkowska, Phys. Rev. B **57**, 14 097 (1998).
- ³² M.D. Lumsden, B.D. Gaulin, H. Dabkowska, and M.L. Plumer, Phys. Rev. Lett. **76**, 4919 (1996).
- ³³ D.E. Moncton, R.J. Birgeneau, L.V. Interrante, and F. Wudl, Phys. Rev. Lett. **39**, 507 (1977).
- ³⁴ M.N. Popova, A.B. Sushkov, S.A. Golubchik, A.N. Vasil'ev, and L.I. Leonyuk, Phys. Rev. B **57**, 5040 (1998).
- ³⁵ For a detailed description of the backward wave oscillator and its use in (sub)mm spectroscopy on solids, see G. Kozlov, and A. Volkov, "Coherent Source Submillimeter Wave Spectroscopy" in *Millimeter Wave Spectroscopy on Solids*, G. Grüner ed. (Springer Verlag, 1995).
- ³⁶ M. Braden, B. Hennion, W. Reichardt, G. Dhalenne, and A. Revcolevschi, Phys. Rev. Lett. **80**, 3634 (1998).
- ³⁷ G. Li, J.L. Musfeldt, Y.J. Wang, S. Jandl, M. Poirier, A. Revcolevschi, and G. Dhalenne, Phys. Rev. B **54**, R15 633 (1996).
- ³⁸ M. Aïn, J.E. Lorenzo, L.P. Regnault, G. Dhalenne, A. Revcolevschi, B. Hennion, and Th. Jolicœur, Phys. Rev. Lett. **78**, 1560 (1997).
- ³⁹ M. Arai, M. Fujita, M. Motokawa, J. Akimitsu, and S.M. Bennington, Phys. Rev. Lett. **77**, 3649 (1996).
- ⁴⁰ H. Kuroe, T. Sekine, M. Hase, Y. Sasago, K. Uchinokura, H. Kojima, I. Tanaka, and Y. Shibuya, Phys. Rev. B **50**, R16 468 (1994).
- ⁴¹ P.H.M. van Loosdrecht, J.P. Boucher, and G. Martinez, G. Dhalenne, and A. Revcolevschi, Phys. Rev. Lett. **76**, 311 (1996).
- ⁴² P.H.M. van Loosdrecht, J. Zeman, G. Martinez, G. Dhalenne, and A. Revcolevschi, Phys. Rev. Lett. **78**, 487 (1997).
- ⁴³ A. Damascelli, D. van der Marel, M. Grüniger, C. Presura, T.T.M. Palstra, J. Jegoudez, and A. Revcolevschi, Phys. Rev. Lett. **81**, 918 (1998).
- ⁴⁴ A. Damascelli, D. van der Marel, J. Jegoudez, G. Dhalenne, and A. Revcolevschi, Physica B, in press (1999).
- ⁴⁵ P.H.M. van Loosdrecht, S. Huant, G. Martinez, G. Dhalenne, and A. Revcolevschi, Phys. Rev. B **54**, R3730 (1996).
- ⁴⁶ G.S. Uhrig, Phys. Rev. Lett. **79**, 163 (1997).

- ⁴⁷ I. Yamada, M. Nishi, and J. Akimitsu, *J. Phys.* **8**, 2625 (1996).
- ⁴⁸ M. Hidaka, M. Hatae, I. Yamada, M. Nishi, and J. Akimitsu, *J. Phys.* **9**, 809 (1997).
- ⁴⁹ L.P. Regnault, J.-P. Renard, G. Dhahlenne, and A. Revcolevschi, *Europhys. Lett.* **32**, 579 (1995).
- ⁵⁰ Y. Sasago, N. Koide, K. Uchinokura, M.C. Martin, M. Hase, K. Hirota, and G. Shirane, *Phys. Rev. B* **54**, R6835 (1996).
- ⁵¹ H. Nakao, M. Nishi, Y. Fujii, T. Masuda, I. Tsukada, K. Uchinokura, K. Hirota, and G. Shirane, *cond-mat/9811324* (23 November 1998).
- ⁵² B. Grenier, J.-P. Renard, P. Veillet, C. Paulsen, G. Dhahlenne, and A. Revcolevschi, *Phys. Rev. B* **58**, 8202 (1998).
- ⁵³ W. Geertsma, and D. Khomskii, *Phys. Rev. B* **54**, 3011 (1996).
- ⁵⁴ D. Khomskii, W. Geertsma, and M. Mostovoy, *Czech. J. Phys.* **46**, 3239 (1996).
- ⁵⁵ J. Goodenough, *Magnetism and the Chemical Bond* (John Wiley & Sons, New York, 1963).
- ⁵⁶ T. Moriya, *Phys. Rev.* **120**, 91 (1960).
- ⁵⁷ For a review, see M.A. Kastner, R.J. Birgeneau, G. Shirane, and Y. Endoh, *Rev. Mod. Phys.* **70**, 897 (1998), and references therein.
- ⁵⁸ M. Grüninger, Ph.D. Thesis, University of Groningen, in preparation (1999).
- ⁵⁹ M. Grüninger, D. van der Marel, A. Damascelli, A. Zibold, H.P. Geserich, A. Erb, M. Kläser, Th. Wolf, T. Nunner, and T. Kopp, *Physica C*, in press (1999).
- ⁶⁰ G.S. Uhrig, *Phys. Rev. B* **57**, R14004 (1998).
- ⁶¹ C. Gros, and R. Werner, *Phys. Rev. B* **58**, R14677 (1998).
- ⁶² B. Büchner, U. Ammerahl, T. Lorenz, W. Brenig, G. Dhahlenne, and A. Revcolevschi, *Phys. Rev. Lett.* **77**, 1624 (1996).
- ⁶³ T. Lorenz, B. Büchner, P.H.M. van Loosdrecht, F. Schönfeld, G. Chouteau, A. Revcolevschi, and G. Dhahlenne, *Phys. Rev. Lett.* **81**, 148 (1998).
- ⁶⁴ K. Fabricius, A. Klümper, U. Löw, B. Büchner, T. Lorenz, G. Dhahlenne, and A. Revcolevschi, *Phys. Rev. B* **57**, 1102 (1998).
- ⁶⁵ G. Bouzerar, A.P. Kampf, and G.I. Japaridze, *Phys. Rev. B* **58**, 3117 (1998).
- ⁶⁶ G. Castilla, S. Chakravarty, and V.J. Emery, *Phys. Rev. Lett.* **75**, 1823 (1995).
- ⁶⁷ K. Okamoto, and K. Nomura, *Phys. Lett. A* **169**, 433 (1993).
- ⁶⁸ J. Riera, and A. Dobry, *Phys. Rev. B* **51**, 16098 (1995).
- ⁶⁹ G. Bouzerar, A.P. Kampf, and F. Schönfeld, *cond-mat/9701176* (23 January 1997).
- ⁷⁰ B. Büchner, H. Fehske, A.P. Kampf, and G. Wellein, *Physica B* **259-261**, 956 (1999).
- ⁷¹ G. Wellein, H. Fehske, and A.P. Kampf, *Phys. Rev. Lett.* **81**, 3956 (1998).
- ⁷² J.E. Lorenzo, L.P. Regnault, J.P. Boucher, B. Hennion, G. Dhahlenne, and A. Revcolevschi, *Europhys. Lett.* **45**, 619 (1999).